Mathematical Biosciences 254 (2014) 6–27

Contents lists available at ScienceDirect

Mathematical Biosciences

journal homepage: www.elsevier.com/locate/mbs

A spatial model with pulsed releases to compare strategies for the sterile insect technique applied to the mosquito *Aedes aegypti*

Thomas P. Oléron Evans *, Steven R. Bishop

Department of Mathematics, University College London, Gower Street, London WC1E 6BT, UK
Centre for Advanced Spatial Analysis, UCL Bartlett Faculty of the Built Environment, 90 Tottenham Court Road, London W1T 4TJ, UK

ARTICLE INFO

Article history:
Received 24 April 2013
Received in revised form 27 May 2014
Accepted 2 June 2014
Available online 12 June 2014

Keywords:
Mathematical model
SIT
RIDL
Pulsed releases
Aedes aegypti
Dynamical systems

ABSTRACT

We present a simple mathematical model to replicate the key features of the sterile insect technique (SIT) for controlling pest species, with particular reference to the mosquito *Aedes aegypti*, the main vector of dengue fever. The model differs from the majority of those studied previously in that it is simultaneously spatially explicit and involves pulsed, rather than continuous, sterile insect releases. The spatially uniform equilibria of the model are identified and analysed. Simulations are performed to analyse the impact of varying the number of release sites, the interval between pulsed releases and the overall volume of sterile insect releases on the effectiveness of SIT programmes.

Results show that, given a fixed volume of available sterile insects, increasing the number of release sites and the frequency of releases increases the effectiveness of SIT programmes. It is also observed that programmes may become completely ineffective if the interval between pulsed releases is greater that a certain threshold value and that, beyond a certain point, increasing the overall volume of sterile insects released does not improve the effectiveness of SIT. It is also noted that insect dispersal drives a rapid recolonisation of areas in which the species has been eradicated and we argue that understanding the density dependent mortality of released insects is necessary to develop efficient, cost-effective SIT programmes.

1. Introduction

The sterile insect technique (SIT) is a method for the control or eradication of insect species through the release of large numbers of insects (usually exclusively males) that have been modified to reduce their reproductive success. The insects may be exposed to radiation, infected with bacteria or, in a variation known as RIDL (released insects with a dominant-lethal), genetically modified to be dependent on a chemical that is not available in their natural environment. Whichever technique is employed, the objective is that modified insects will mate with wild insects, but that their offspring will be largely non-viable. This technique has been successfully used to eradicate or suppress many species of insect in various environments around the world and remains in operation on large scales, with some facilities capable of producing around two billion sterile insects per week for SIT programmes [1].

The mosquito *Aedes aegypti* is the main vector of dengue fever, a potentially fatal disease with 50–100 million cases per year, for which there is no approved vaccine or medication [2]. Several authors have advocated SIT as a means to control populations of mosquito species and thus to address the threat of dengue fever and other diseases [1,3], though others have argued that *Aedes aegypti* may not be suitable for an SIT programme owing to the dispersal and distribution characteristics of the species [4]. While previous attempts to apply SIT to mosquito species have been successful against isolated populations, they have been unsuccessful on larger scales, partly because the techniques used to sterilise males have often reduced their fitness to mate with wild females. However, modern transgenic techniques may have the potential to overcome these issues [5].

Predicting the outcome of SIT programmes is extremely important to ensure that they are practical, affordable and effective and several mathematical models have been presented to simulate the application of the technique to *Aedes aegypti*. Several authors have created extremely detailed models that take into account the multiple stages of the mosquito's development, the varying gonotrophic cycle of the female (the feeding and reproductive cycle) and diverse environmental factors. A detailed review of the mathematical modelling of mosquito populations

* Corresponding author at: Department of Mathematics, University College London, Gower Street, London WC1E 6BT, UK. Tel.: +44 (0)20 3108 3877; fax: +44 (0)20 3108 3258.
E-mail addresses: thomas.evans.11@ucl.ac.uk (T.P. Oléron Evans), s.bishop@ucl.ac.uk (S.R. Bishop).

http://dx.doi.org/10.1016/j.mbs.2014.06.001
0025-5564/

(particularly *Aedes aegypti*), their role in spreading dengue fever and the effect of SIT is presented in Section 2.

In this paper, we present a simple model of the population dynamics of *Aedes aegypti* and the effects of SIT on the species. Unlike the vast majority of those that have previously been studied, the model is both spatially explicit and involves pulsed (rather than continuous) sterile insect releases. This lends it the flexibility to simulate a wide range of spatial and temporal sterile insect release strategies for *Aedes aegypti*, which have not previously been investigated in a systematic way.

Following the review of previous modelling approaches in Section 2, the model is defined in Section 3 and certain equilibria of the dynamics are analysed in Section 4. Section 5 discusses how the parameters of the model were chosen to represent an SIT programme for *Aedes aegypti* with the subsequent analysis of different release strategies presented in Section 6. A discussion of the strengths and weaknesses of the model and of possible directions for future research is presented in Section 7, with the main conclusions of the paper listed in Section 8. A brief comparison of alternative sterile insect release patterns can be found in Appendix A.

All simulations presented in this paper were programmed in Python [6], using NumPy [7], with visualisations created using Matplotlib [8].

2. Dynamical models of mosquito populations, dengue transmission and control strategies

Unless otherwise stated, the models discussed in this section relate exclusively to the mosquito *Aedes aegypti*. However, certain sources that focus on other species have been included where their results were judged to be particularly relevant to our work.

2.1. Non-spatial models of mosquito population dynamics

The simplest dynamical population models of *Aedes aegypti* and other insect populations are simulated dynamic life tables. These are essentially non-spatial discrete-time dynamical systems, in which the dynamical variables represent the sizes of various subpopulations of the insect species (e.g. eggs, larvae, mature females), tracked by cohort, with the rates of transition between these subpopulations at each time step defined by means of dynamical equations. These equations may be extremely complex, involving many separate biological and physical processes, and are generally dependent on parameters that represent characteristics of the insects (e.g. oviposition rate, mortality) and the habitat (e.g. temperature, number and type of available oviposition sites, predation). The parameters may vary both seasonally and stochastically, though the population dynamics themselves are otherwise intrinsically deterministic [9].

An early example of such a dynamical system model for *Aedes aegypti* was presented by Birley [10], who showed that models of this type could be used to understand the statistical variability of the rates of development of different individual insects. Many later dynamic life table simulations of *Aedes aegypti* are based on the 'container inhabiting mosquito simulation model' (CIMSiM) of Focks et al. [11], which incorporates numerous factors affecting the population dynamics such as the gonotrophic cycle of the female, the influence of weather and the depletion of food supplies [12].

Maguire et al. [13] used CIMSiM to compare potential control strategies for *Aedes aegypti*, commenting that "simulation modelling...may never be sophisticated enough to be used as a forecasting tool..." and identifying the true role of such models as determining the "most effective combination and timing of control methods and...areas at highest risk of having large *Aedes aegypti* populations.".

More recently, Williams et al. [14] successfully used CIMSiM to estimate and predict the size and structure of *Aedes aegypti* populations in Queensland, Australia, while Morin and Comrie [15] created the related 'dynamic mosquito simulation model' (DyMSiM) to investigate the possible effects of climatic changes on populations of another mosquito species, *Culex quinquefasciatus* (a vector of West Nile virus).

Alternative discrete-time dynamical models to CIMSiM include TAENI2 [16], a biologically detailed simulation model of the black salt marsh mosquito, *Aedes taeniorhynchus*. Though the model is essentially non-spatial, insect immigration and emigration are included as exogenous processes, and the authors observe that mosquito dispersal can lead to rapid recolonisation of areas in which the species had previously been eradicated.

Another approach was presented by Otero et al. [9], who modelled the life cycle of *Aedes aegypti* as a Markov chain, using their model to establish a criterion for *Aedes aegypti* persistence in urban environments.

2.2. Spatial models of mosquito population dynamics

The most common means of creating a spatially explicit mosquito population dynamical model has been to run a large number of discrete-time dynamical models of the sort described in the previous section in parallel over a lattice of cells, introducing diffusion-type dynamics to model mosquito dispersal.

This was the approach employed by Otero et al. [17], when developing a spatially explicit version of their earlier model, claiming that they had created "the first stochastic spatial model for *Aedes aegypti* populations based on the life cycle of the mosquito and its dispersal". Their conclusion, that the observed dynamics of the species in Buenos Aires, Argentina, could be explained by a complex process of local eradication, dispersal and recolonisation, recalls that of Ritchie and Montague [16]. The Otero et al. [17] model was recently refined further to introduce more detailed hatching and pupation processes [18].

In a similar way, Legros et al. [19] developed a spatial simulation of *Aedes aegypti* population dynamics, 'Skeeter Buster', which built on CIMSiM, incorporating additional stochasticity, breeding container scale spatial structure and a lattice of cells representing individual houses. The model was able to broadly replicate the observed population dynamics of *Aedes aegypti* in Iquitos, Peru, and Buenos Aires over periods of a year or more.

A potentially more sophisticated approach to the spatial modelling of mosquito population dynamics is to replace the discrete-time component of these lattice models with a continuous-time version, based on ordinary differential equations (ODEs). One such approach is proposed by Mageni Lutambi et al. [20], who create a detailed mosquito dispersal model over a hexagonal lattice, taking into account heterogeneously distributed resources (e.g. human hosts or oviposition sites), and use it to demonstrate that such heterogeneity in the environment can have a complex effect on the population dynamics of a species.

One of the relatively few true agent-based approaches to spatial modelling of *Aedes aegypti* is *SimPopMosq* [21], a highly detailed, spatially and temporally discrete model with agents representing mosquitoes, humans and other mammals as well as inanimate objects such as water containers. These agents interact over a rectangular cellular lattice and emit traces (such as odours) which diffuse across space, while mosquito agents have a number of developmental stages and can adopt a variety of behaviour patterns. The authors reported high levels of similarity between *SimPopMosq* simulations and experimental data.

The majority of spatially explicit simulations of *Aedes aegypti*, however, are not pure population dynamical models, but incorporate additional factors, such as dengue transmission and explicit

modelling of SIT. These include a number of models that are continuous in time and space, based on partial differential equations (PDEs), some of which are mentioned in the forthcoming sections.

2.3. Models incorporating dengue transmission

As *Aedes aegypti* is a principal vector of dengue fever, mathematical models of the coupled dynamics of mosquito populations, human populations and the dengue virus can be a valuable public health tool. One such model combines CIMSiM, representing the dynamics of the mosquito population, with a Dengue Transmission Model (DENSiM), a non-spatial individual-based model of human population dynamics and multiple strains of the dengue virus. This model has been recommended by the United Nations [12] for optimising dengue control strategies and evaluating the impact of climate change and has been used to identify the most important factors affecting dengue transmission [22].

Other spatial models of dengue transmission have built on the spatial model of Otero et al. [17]. For example, Barmak et al. [23] propose an individual-based model of mosquito and human populations, over a cellular lattice representing heterogeneous city blocks in Buenos Aires. In this model, while mosquitoes move according to the same diffusion-type process described by Otero et al. [17], the movement of human agents is based on detailed research, with complex mobility networks, commuting and Lévy flights. The authors identify long-distance human mobility as a key factor in accelerating the spread of dengue outbreaks.

Otero and Solari [24] also extended the Otero et al. [17] model to incorporate dengue transmission, coupling it with an SEIR (susceptible–exposed–infected–recovered) dynamical system model of dengue infection in humans to evaluate different epidemic scenarios.

Additional work on the modelling of dengue transmission includes that of Favier et al. [25], in which SEI models of *Aedes aegypti* dynamics within households are coupled with spatial and non-spatial individual based SEIR models of human dynamics between households, and that of Tran and Raffy [26], which also uses a coupled SEI/SEIR approach, but includes the movement of *Aedes aegypti* as a spatial diffusion process and does not explicitly model the movement of human hosts.

2.4. Non-spatial sterile insect models

Several authors have expanded non-spatial discrete population dynamical models to model SIT and RIDL control programmes. One of the earliest to be investigated using computer simulation was that of Curtis et al. [27], who compared experimental data from caged *Aedes aegypti* mosquitoes with simulated releases of sterile males and 'distorter males' (that produce lower ratios of female offspring), to identify the more effective intervention.

This work was followed by that of Itô [28] and Itô and Kawamoto [29], who combined a discrete-time logistic model of melon fly (*Dacus cucurbitae*) population growth with a Poisson-binomial model of matings. This model was used to predict the necessary ratios of sterile to healthy insects for species eradication, but the authors noted that their results were far more optimistic than the ratios required in practice. As in the later work of Ritchie and Montague [16] and Otero et al. [17], spatial effects that could not be captured by the model were proposed as a reason for this discrepancy, specifically insect dispersal and recolonisation of treated areas.

More recent non-spatial approaches to modelling SIT have been based on systems of ODEs. For example, Barclay and Mackauer [30] considered a logistic population model to compare the effectiveness of sterile male, sterile female and mixed gender SIT release programmes and to identify threshold populations for species eradication. Another SIT model of this type, based on the Lotka–Volterra equations, was considered by Harrison et al. [31] to analyse pest populations subject to predation.

Esteva and Yang [32] analysed an ODE model of SIT to determine equilibria and bifurcations for the population dynamics of *Aedes aegypti*, with particular reference to parameters governing the reproductive rate, the ratio of sterile to healthy males and the rate of sterile releases. A more detailed system of time delayed ODEs, combined with an SIR-like compartmental epidemiolgical model, was considered by Alphey et al. [33] and used to assess the effectiveness of RIDL programmes for *Aedes aegypti*, concluding that the cost of such programmes would be lower than the financial burden directly and indirectly imposed by the disease.

2.5. Spatial sterile insect models

Much of the most recent work on the modelling of sterile insect methods has involved spatially explicit models, some of which have been based on the principle of parallel discrete-time dynamical systems over cellular lattices, as discussed in Section 2.2. For example, Yakob and Bonsall [34] considered a model of this type to investigate RIDL control strategies, initiating their simulations at the non-zero equilibrium of the wild population to represent the control of an established pest species and considering uniform releases of sterile insects across all cells in the target area. Once again, results suggested that high rates of insect dispersal reduce the effectiveness of control strategies.

Similar techniques were employed by Potgieter et al. [35] to model SIT control of the moth *Eldana saccharina* by means of a cellular discrete-time reaction–diffusion model. Unlike the approach of Yakob and Bonsall [34], however, this model did not assume spatially uniform sterile insect releases, but supposed that releases only occurred along particular strips of the region, thus modelling releases from a vehicle travelling along particular paths through the target area. The authors concluded that optimal release strategies were highly dependent on factors including dispersal rates and sterile insect release rates.

Another attempt to understand the effect of the spatial distribution of release sites in RIDL programmes for *Aedes aegypti* was produced by Legros et al. [36], who used their 'Skeeter Buster' model, parameterised to represent Iquitos, Peru, to compare uniform spatial release strategies with strategies involving releases at discrete locations, either chosen randomly or spread evenly across the simulation region. While observing that total eradication of the target population was potentially unrealistic owing to spatial heterogeneity, they concluded that evenly spread release sites were more effective than randomly chosen sites.

An alternative strategy for spatially explicit SIT modelling is to use PDEs. The work of Manoranjan and van den Driessche [37] is an early example of such an approach, in which the ODE model of Barclay and Mackauer [30] is expanded to a spatial PDE model through the introduction of a diffusion-like insect dispersal process. The spatial nature of this model allowed the authors to consider SIT techniques over a heterogeneous environment and to consider spatially non-uniform sterile insect releases, as Potgieter et al. [35] had done.

In contrast, Li and Zou [38] studied a highly abstract one-dimensional PDE model of SIT, in which sterile insects are released at the boundaries of an interval, identifying the volume of sterile releases required for species eradication in this setting.

One of the most novel approaches to spatial SIT modelling was provided by Ferreira et al. [4], who produced a cellular automata model of sterile insect control of *Aedes aegypti* over a rectangular lattice and considered the dynamics of the species for different spatial distributions of breeding sites. This is both one of the only true cellular automata models of SIT and one of the only models in

which sterile male releases occur at random locations, rather than uniformly across space or at specified locations. From simulations of the model, the authors identified spatial heterogeneity of the environment as having a significant impact of the effectiveness of SIT programmes.

One of the few true agent-based spatial models of SIT for *Aedes aegypti* was presented by [39]. The model is similar to the later simulation of de Almeida et al. [21] (which did not involve sterile insect releases), in that it is built on a rectangular lattice, features versatile agents representing mosquitoes and humans and includes elements that diffuse across space, such as pheromones and humidity. However, the authors acknowledge that the model is not complete and would require further modifications to improve its applicability.

2.6. Sterile insect models with pulsed releases

In all the above SIT models, sterile insect releases occur at a uniform rate, at least to the degree of temporal discretisation of the model. Few models have been proposed in which sterile releases occur in discrete pulses, despite the fact that such release strategies are more realistic.

One exception is a time-delayed, non-spatial ODE model, presented by White et al. [40], parametrised for *Aedes aegypti*. The authors use their model to demonstrate that small, frequent releases are more effective than larger, less frequent releases, going on to remark that "models that assume a constant release strategy will tend to over-estimate the true level of population control."

Another non-spatial ODE SIT model with pulsed releases, composed of coupled SIR-type models for the mosquito and human populations, was proposed for the Asian tiger mosquito *Aedes albopictus* by Dumont and Tchuenche [41]. The conclusions from this work were in line with those of White et al. [40], that small, frequent pulsed releases were most effective.

Very few explicitly spatial models are known to have been used to study SIT techniques with pulsed sterile insect release. One exception is the recent work of Dufourd and Dumont [42,43], in which a biologically detailed continuous spatial (PDE) model of the dynamics of *Aedes albopictus*, is used to examine the most effective strategies for SIT control programmes with pulsed releases. The main focus of this work is the effect of environmental heterogeneity, particularly in the distribution of breeding and feeding sites and the wind direction, and temporal heterogeneity (seasonal temperature variation) on the dynamics of the species and the effect of such heterogeneity on potential control programmes. The work also includes some comparison of SIT strategies in terms of the time between pulsed releases and the optimal location of releases with reference to the prevailing wind direction.

Significant conclusions of this work include the observations that understanding the effect of environmental heterogeneity is necessary for the development of successful SIT programmes, thus supporting the case for spatial over non-spatial models, and that smaller and more frequent releases are more efficient than larger and less frequent releases, further supporting the work of White et al. [40] and Dumont and Tchuenche [41] (albeit from a model of a different species of mosquito).

3. An SIT model for *Aedes aegypti*

3.1. Motivations

Considering the literature on modelling mosquito dynamics as a whole, two key factors may be identified that have been observed to have a significant effect on the efficacy of SIT programmes in simulations: mosquito dispersal, through which healthy insects are able to rapidly recolonise areas that have been cleared by SIT or other control programmes; and pulsed rather than continuous sterile insect releases, a practical necessity in real world applications of SIT. Analysis of these two factors and the relationship between them demands the study of a spatially explicit model with a pulsed release strategy, something that has received very little consideration by previous authors, particularly for the mosquito *Aedes aegypti*.

The primary goal, therefore, is to present and analyse a simple model that replicates the essential features of SIT in *Aedes aegypti* without detailed reference to the precise biology of the species, but which is both spatially explicit and capable of simulating pulsed sterile insect releases. Naturally, the complexity of the model may be increased in later work through the reintroduction of more detailed biological information, when the essential influence of the key spatial and temporal factors has been understood.

In line with the conclusions of Maguire et al. [13] on the value of such models, the aim is not to create a tool capable of precise forecasting for specific SIT implementations, but to broadly assess the likely impact of simultaneously varying certain factors that have been seen to affect the efficacy of SIT programmes, including the number of sites at which sterile insects are released, the interval between pulsed releases, and the overall volume of sterile insect releases.

The results obtained from simulations of this model will be compared with those derived from other models, which may include more biological detail (with particular reference to the recent spatial pulsed SIT models of *Aedes albopictus* from Dufourd and Dumont [42,43]), to determine whether the relatively simple assumptions underlying it are capable of producing interesting and valuable conclusions.

3.2. General features

The model we propose follows similar principles to those of Legros et al. [19], Barmak et al. [23], Otero and Solari [24], Yakob and Bonsall [34], and Potgieter et al. [35], in that it comprises many discrete-time dynamical systems run in parallel over a cellular lattice, with local interactions between cells to model insect dispersal.

Three subpopulations of insects are considered: healthy female mosquitoes, healthy male mosquitoes and sterile male mosquitoes. Unlike previous similar models, which were based on rectangular lattices, the environment is modelled as a hexagonal lattice to provide more even dispersal of mosquitoes over small time increments, in order that dispersal between frequent pulsed releases may be accurately modelled. The precise size and shape of the lattice may be altered depending on the particular environment to be modelled.

Model time advances in discrete intervals, and dynamical transition rules are applied to the three subpopulations in each cell. Formally, $x_{i,t}$, $y_{i,t}$ and $z_{i,t}$ represent the per-cell population densities of healthy female, healthy male and sterile male mosquitoes in cell i at time t. Note that, to ensure the simplicity of the model, these variables are not constrained to take integer values.

The transition rules calculate dispersal, mortality and reproduction sequentially as separate processes. Clearly, this is a simplification of the true dynamics, since we would not expect these processes to occur separately in reality.

The different variables and their meanings are summarised in Fig. 1.

3.3. Dispersal

In common with the models of Otero et al. [17], Barmak et al. [23], and Potgieter et al. [35], among others, individual insects are assumed to move to adjoining cells according to a random

walk. Justification for this process as a basis for mosquito movement in the absence of other stimuli may be found in the work of Daykin et al. [44], who state that mosquitoes may be assumed to move in a random direction in such circumstances, and that of Otero et al. [17], who observe that many experiments (though not all) show very short dispersal of *Aedes aegypti*, suggesting that restricting movement to occur between neighbouring cells should therefore be reasonable, provided that the spatial scale of the model is carefully chosen (see Section 5.2).

We suppose that individuals remain in their current cell i with probability p and move to any particular neighbouring cell with probability $(1-p)/|N(i)|$, where $N(i)$ is the open neighbourhood of i, the set of all cells adjacent to i. In an infinite hexagonal lattice, $|N(i)| = 6$ for all cells. The aggregated dispersal of the mosquitoes is therefore a diffusion-like process, in common with that of many previous models (see Sections 2.2, 2.3 and 2.5).

The density of individuals of each type in cell i at time t, after dispersal has been accounted for, is thus given by the following equations:

$$\begin{aligned}\overline{x}_{i,t} &= px_{i,t-1} + (1-p)\sum_{j\in N(i)}\frac{x_{j,t-1}}{|N(j)|}\\ \overline{y}_{i,t} &= py_{i,t-1} + (1-p)\sum_{j\in N(i)}\frac{y_{j,t-1}}{|N(j)|}\\ \overline{z}_{i,t} &= pz_{i,t-1} + (1-p)\sum_{j\in N(i)}\frac{z_{j,t-1}}{|N(j)|}\end{aligned} \tag{1}$$

3.4. Mortality

To model mosquito mortality, we suppose that a certain proportion of insects present in i at time $t-1$ will not survive to time t. As in a logistic growth model, this proportion will depend on the total population of i, with high mosquito density leading to an increased mortality rate due to increased competition for resources (for more detailed discussion of density dependent mortality in relation to *Aedes aegypti* and in other SIT models, see [9,19,30]).

We also suppose that each subpopulation has a certain baseline survival rate, $\alpha, \beta, \gamma \in [0,1]$, the respective probabilities that an individual from each group will survive from time $t-1$ to time t when the population density is low enough that there is no competition for resources.

Letting $\overline{X}_{i,t} = \overline{x}_{i,t} + \overline{y}_{i,t} + \overline{z}_{i,t}$, we suppose that the decrease in each of the subpopulation in i at time t due to mortality is given by the expressions:

$$\begin{aligned}&\overline{x}_{i,t}[(1-\alpha) + \alpha F(\overline{X}_{i,t})]\\ &\overline{y}_{i,t}[(1-\beta) + \beta F(\overline{X}_{i,t})]\\ &\overline{z}_{i,t}[(1-\gamma) + \gamma F(\overline{X}_{i,t})]\end{aligned} \tag{2}$$

where F is a function representing mortality due to density dependence.

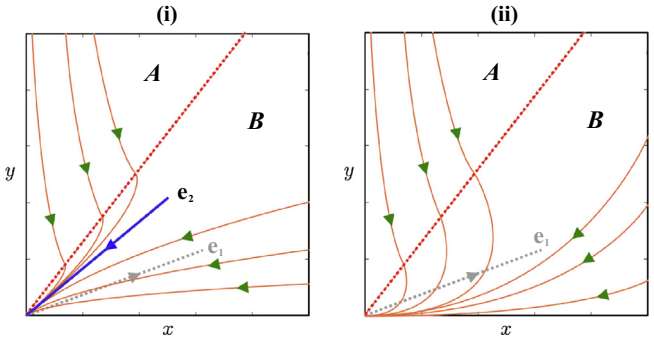

Fig. 2. The dynamics of a dual case The diagrams show the two possible dynamical behaviours of the dual case in which $(0,0)$ is 'unstable' in region A and 'stable' in region B. Regions A and B are divided by the interface $y = (\alpha/\beta)\hat{m}x$. **(i)** (36) false: $\mathbf{e}_1$ (dotted) and $\mathbf{e}_2$ are directed into region B. **(ii)** (36) true: $\mathbf{e}_1$ (dotted) is directed into region B and $\mathbf{e}_2$ has non-positive gradient.

Ideally, we would choose F based on our insight into the biological processes involved. However, the precise form of the function is unknown, so in order to gain an understanding of the dynamics, we choose a generic function with the following features (the subscripts i and t have been removed for the sake of clarity):

1. $F(\overline{X})$ should be continuous and increasing $\forall \overline{X} \geqslant 0$,
2. $F(\overline{X}) \in [0,1], \forall \overline{X} \geqslant 0$,
3. $F(0) = 0$ and $F(\overline{X}) \to 1$ as $\overline{X} \to \infty$.

Condition 1 ensures that greater population densities result in higher mortality and that this relationship is continuous. Condition 2 ensures that the number of deaths in each group is non-negative and does not exceed the size of the subpopulation. Condition 3 ensures both that mortality due to competition is negligible for sufficiently low population densities and that there is no upper bound on the proportion of the population that may die owing to competition as the density increases.

We choose:

$$F(\overline{X}) = \frac{\overline{X}}{C+\overline{X}},\ C > 0 \tag{3}$$

which clearly satisfies the necessary conditions. Observe that (3) is related to the Monod equation of microbial growth [45].

C is a parameter that can be interpreted as controlling the number of mosquitoes that can be supported by a single unit of area. Specifically, C is the population density (after dispersal) at which, at a given iteration and in a given cell, precisely half of all mosquitoes will die from overcrowding. In regions in which the terrain is not homogenous, this parameter may vary from location to location, but the analysis of such situations is beyond the scope of this paper.

We therefore have the following equations to describe the surviving population in cell i at time t:

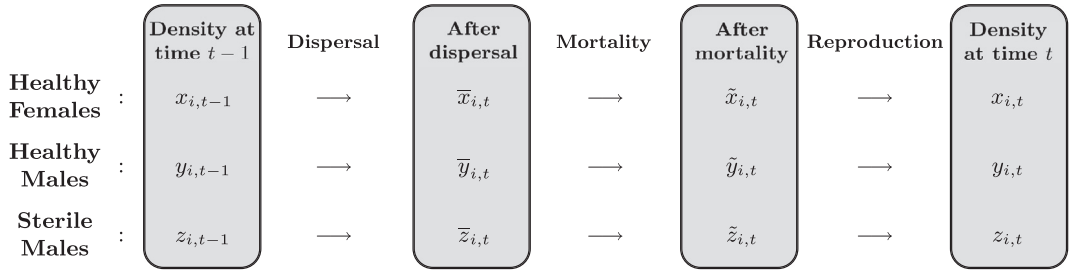

Fig. 1. Diagram showing the events considered by the model over a single time interval and the meanings of the different variables used at each stage of the process.

$$\begin{aligned}\tilde{x}_{i,t} &= \overline{x}_{i,t}\alpha[1-F(\overline{X}_{i,t})]\\ \tilde{y}_{i,t} &= \overline{y}_{i,t}\beta[1-F(\overline{X}_{i,t})]\\ \tilde{z}_{i,t} &= \overline{z}_{i,t}\gamma[1-F(\overline{X}_{i,t})]\end{aligned} \tag{4}$$

3.5. Reproduction

We assume that, in the absence of sterile males, there is an optimal ratio $\hat{m}$ of healthy males to healthy females, at which females can reproduce at their maximum biological rate, $\hat{b}$ healthy offspring per female per time interval, and that when only healthy insects are present the relationship between the actual ratio of males to females $m_{i,t}$ and the actual rate of production of healthy offspring per female per time interval $b_{i,t}$ is linear for $m_{i,t} \leqslant \hat{m}$. However, when sterile males are present, this rate will be reduced, since matings involving such males will be largely unsuccessful.

We suppose that in a cell i, matings involving healthy and sterile males are in the ratio $\tilde{y}_{i,t} : r\tilde{z}_{i,t}$, where r is the coefficient of reduced mating competitive ability of sterile males [40]. Generally, $r < 1$ since the procedures used to modify the sterile males also reduce their reproductive success [1]. If we further assume that a low proportion $v \in [0,1]$ of the offspring of sterile males are viable (the basis of the SIT and RIDL techniques), neglecting the subscripts i,t for clarity and having already reduced the population due to mortality, we have that the number of healthy offspring produced in i at time t is given by:

$$B(\tilde{x},\tilde{y},\tilde{z}) = \begin{cases} \tilde{x}\hat{b}\left(\frac{\tilde{y}}{\tilde{y}+r\tilde{z}} + v\frac{r\tilde{z}}{\tilde{y}+r\tilde{z}}\right)\left(\frac{\tilde{y}+r\tilde{z}}{\hat{m}\tilde{x}}\right), & \tilde{y}+r\tilde{z} < \hat{m}\tilde{x} \\ \tilde{x}\hat{b}\left(\frac{\tilde{y}}{\tilde{y}+r\tilde{z}} + v\frac{r\tilde{z}}{\tilde{y}+r\tilde{z}}\right), & \text{otherwise}\end{cases}$$

This can be simplified to the following form, from which it can be seen that the first case is limited by the size of the sexually active male population $\tilde{y}+r\tilde{z}$, while the second case is limited by the size of the female population $\tilde{x}$:

$$B(\tilde{x},\tilde{y},\tilde{z}) = \begin{cases} \frac{\hat{b}}{\hat{m}}(\tilde{y}+vr\tilde{z}), & \tilde{y}+r\tilde{z} < \hat{m}\tilde{x} \\ \tilde{x}\hat{b}\left(\frac{\tilde{y}+vr\tilde{z}}{\tilde{y}+r\tilde{z}}\right), & \text{otherwise}\end{cases} \tag{5}$$

To simplify the model, we assume that the delay from fertilisation to oviposition is negligible and that viable offspring immediately become sexually mature adults.

Setting $g \in (0,1)$ equal to the mean proportion of offspring that are male, the equations governing the change in the populations of each type of mosquito in i at time t can be written:

$$\begin{aligned}x_{i,t} &= \tilde{x}_{i,t} + (1-g)B(\tilde{x}_{i,t},\tilde{y}_{i,t},\tilde{z}_{i,t})\\ y_{i,t} &= \tilde{y}_{i,t} + gB(\tilde{x}_{i,t},\tilde{y}_{i,t},\tilde{z}_{i,t})\\ z_{i,t} &= \tilde{z}_{i,t}\end{aligned} \tag{6}$$

3.6. Equilibria of the healthy population

A derivation of these results presented in this section and visual representations of the bifurcations described (Figs. 5 and 6) can be found in Section 4.

Under the dynamics of the model, in the absence of sterile males, for cells sufficiently far from the boundary, the healthy population $(x_{i,t}, y_{i,t})$ tends to an equilibrium (x^*, y^*), where x^* and y^* depend on the values of the parameters. There are three possible cases:

1. If:

$$\hat{b} \leqslant \max\left[\frac{1}{1-g}\left(\frac{1}{\alpha}-1\right), \frac{\hat{m}}{g}\left(\frac{1}{\beta}-1\right)\right]$$

then $(0,0)$ is the only equilibrium. It is a global attractor and any healthy population will tend to extinction.

2. If:

$$\hat{b} > \max\left[\frac{1}{1-g}\left(\frac{1}{\alpha}-1\right), \frac{\hat{m}}{g}\left(\frac{1}{\beta}-1\right)\right]$$

and

$$\hat{m} \leqslant \frac{\beta\hat{b}g}{(\alpha-\beta)+\alpha\hat{b}(1-g)}$$

then $(0,0)$ is an unstable equilibrium and any mixed population of healthy males and females tends to the following stable equilibrium:

$$\begin{aligned}x^* &= C\left[\frac{(\alpha-\beta)+\alpha\hat{b}(1-g)}{(\alpha-\beta)+\alpha\hat{b}}\right]\left[\alpha(1+\hat{b}(1-g))-1\right]\\ y^* &= C\left[\frac{\alpha\hat{b}g}{(\alpha-\beta)+\alpha\hat{b}}\right]\left[\alpha\left(1+\hat{b}(1-g)\right)-1\right]\end{aligned} \tag{7}$$

3. If:

$$\hat{b} > \max\left[\frac{1}{1-g}\left(\frac{1}{\alpha}-1\right), \frac{\hat{m}}{g}\left(\frac{1}{\beta}-1\right)\right]$$

and

$$\hat{m} > \frac{\beta\hat{b}g}{(\alpha-\beta)+\alpha\hat{b}(1-g)}$$

then $(0,0)$ is an unstable equilibrium and any mixed population of healthy males and females tends to the following stable equilibrium:

$$\begin{aligned}x^* &= C\left[\frac{\beta\frac{\hat{b}}{\hat{m}}(1-g)}{(\beta-\alpha)+\beta\frac{\hat{b}}{\hat{m}}}\right]\left[\beta\left(1+g\frac{\hat{b}}{\hat{m}}\right)-1\right]\\ y^* &= C\left[\frac{(\beta-\alpha)+\beta\frac{\hat{b}}{\hat{m}}g}{(\beta-\alpha)+\beta\frac{\hat{b}}{\hat{m}}}\right]\left[\beta\left(1+g\frac{\hat{b}}{\hat{m}}\right)-1\right]\end{aligned} \tag{8}$$

Evidently, any population involving only one gender will tend to extinction in all circumstances.

These results demonstrate the existence of a bifurcation at:

$$\hat{b} = \max\left[\frac{1}{1-g}\left(\frac{1}{\alpha}-1\right), \frac{\hat{m}}{g}\left(\frac{1}{\beta}-1\right)\right]$$

where the stable equilibrium at $(0,0)$ splits into a stable equilibrium (x^*, y^*) and an unstable equilibrium at $(0,0)$ as $\hat{b}$ increases.

4. Mathematical analysis of the model

4.1. Locating spatially uniform equilibria

A spatially uniform equilibrium of the model (on an infinite lattice) is a state in which the values of $x_{i,t}, y_{i,t}, z_{i,t}$ are constant (equal to x^*, y^*, z^*, say) over all cells i and at all times t. At such an equilibrium, by symmetry it is clear that dispersal effects can be neglected and analysis reduced to a single cell. It is also clear that $z^* = 0$, since any non-zero population of sterile males is strictly decreasing due to mortality. We therefore restrict our analysis to the two-dimensional system representing the healthy population before the commencement of a sterile insect programme.

Let m^* be the ratio of males to females at a particular spatially uniform equilibrium. The population vector for a single cell at such an equilibrium can then be written as (x^*, m^*x^*) and, by (6), we have:

$$x^* = \tilde{x}^* + (1-g)B(\tilde{x}^*, \tilde{y}^*, 0)$$
$$m^* x^* = \tilde{y}^* + gB(\tilde{x}^*, \tilde{y}^*, 0)$$

where $\tilde{x}^*$ and $\tilde{y}^*$ represent the densities of males and females after mortality (but before reproduction) in this scenario.

By (4), these equations can be rewritten:

$$\begin{aligned} x^* &= x^*\alpha[1 - F((1+m^*)x^*)] + (1-g)B(\tilde{x}^*, \tilde{y}^*, 0) \\ m^* x^* &= m^* x^* \beta[1 - F((1+m^*)x^*)] + gB(\tilde{x}^*, \tilde{y}^*, 0) \end{aligned} \tag{9}$$

It is clear that $x^* = y^* = 0$ is trivially an equilibrium. To find other equilibria, there are two possible cases to consider. First, we consider the case in which, after mortality has been calculated, there is no deficit of males: $\tilde{y}^*/\tilde{x}^* \geqslant \hat{m}$. By (5), after rearranging and simplifying, (9) becomes:

$$1 = \alpha[1 - F((1+m^*)x^*)][1 + \hat{b}(1-g)] \tag{10}$$
$$m^* = [1 - F((1+m^*)x^*)][m^*\beta + \alpha\hat{b}g] \tag{11}$$

and (10) can be rearranged to give:

$$F((1+m^*)x^*) = 1 - \frac{1}{\alpha}\left[\frac{1}{1+\hat{b}(1-g)}\right] \tag{12}$$

Substituting into (11), we find that the ratio of males to females is:

$$m^* = \left[\frac{1}{g}\left[1 + \frac{1}{\hat{b}}\left(1 - \frac{\beta}{\alpha}\right)\right] - 1\right]^{-1} \tag{13}$$

Finally, using (12), (13) and the definition of F, we find that:

$$\begin{aligned} x^* &= C\left[\frac{(\alpha-\beta) + \alpha\hat{b}(1-g)}{(\alpha-\beta) + \alpha\hat{b}}\right]\left[\alpha\left(1 + \hat{b}(1-g)\right) - 1\right] \\ y^* &= C\left[\frac{\alpha\hat{b}g}{(\alpha-\beta) + \alpha\hat{b}}\right]\left[\alpha\left(1 + \hat{b}(1-g)\right) - 1\right] \end{aligned} \tag{14}$$

The second case is that in which there is a deficit of males after mortality has been calculated: $\tilde{y}^*/\tilde{x}^* < \hat{m}$. Following a similar method, we have:

$$m^* = \frac{1}{1-g}\left[g + \frac{\hat{m}}{\hat{b}}\left(1 - \frac{\alpha}{\beta}\right)\right] \tag{15}$$

$$\begin{aligned} x^* &= C\left[\frac{\beta\frac{\hat{b}}{\hat{m}}(1-g)}{(\beta-\alpha) + \beta\frac{\hat{b}}{\hat{m}}}\right]\left[\beta\left(1 + g\frac{\hat{b}}{\hat{m}}\right) - 1\right] \\ y^* &= C\left[\frac{(\beta-\alpha) + \beta\frac{\hat{b}}{\hat{m}}g}{(\beta-\alpha) + \beta\frac{\hat{b}}{\hat{m}}}\right]\left[\beta\left(1 + g\frac{\hat{b}}{\hat{m}}\right) - 1\right] \end{aligned} \tag{16}$$

4.2. Validity of spatially uniform equilibria

For each of these two cases to represent a genuine non-trivial equilibrium, three conditions must be satisfied:

1. $\tilde{y}^*/\tilde{x}^* \geqslant \hat{m}$; [for (14)] or $\tilde{y}^*/\tilde{x}^* < \hat{m}$; [for (16)],
2. $m^* > 0$,
3. $x^* + y^* > 0$.

These are necessary and sufficient conditions for the equilibria to exist.

We first demonstrate that it is not possible for both equilibria to exist simultaneously. From (4), we see that $\tilde{y}^*/\tilde{x}^* = m^*(\beta/\alpha)$. Substituting into this expression for the first equilibrium (14), using the appropriate expression for m^* (13), condition 1 becomes:

$$\hat{m} \leqslant \frac{\beta\hat{b}g}{(\alpha-\beta) + \alpha\hat{b}(1-g)},\ (\alpha-\beta) + \alpha\hat{b}(1-g) > 0 \tag{17}$$

For the second equilibrium (16), with a similar substitution of (15), condition 1 becomes:

$$\hat{m} > \frac{\beta\hat{b}g}{(\alpha-\beta) + \alpha\hat{b}(1-g)},\ (\alpha-\beta) + \alpha\hat{b}(1-g) > 0 \tag{18}$$

Hence the existence conditions for each equilibrium are mutually exclusive.

Note that the condition $(\alpha-\beta) + \alpha\hat{b}(1-g) > 0$ is stated for the following reasons:

- $(\alpha-\beta) + \alpha\hat{b}(1-g) < 0$ would imply that the right hand sides of the inequalities for $\hat{m}$ are negative. Since $\hat{m} > 0$, this leads to a clear contradiction in (17). It also leads to a contradiction in the second case, since the inequality would be reversed during the algebraic manipulation required to derive (18).
- $(\alpha-\beta) + \alpha\hat{b}(1-g) = 0$ is not possible at a non-trivial equilibrium. In the first case, substituting this expression into (14) would imply a violation of condition 3. In the second case, substituting (15) into condition 1 leads to a contradiction of the equality.

Now, taking the first case (13, 14), conditions 2 and 3 become:

$$\left.\begin{aligned} \hat{b} &> \tfrac{1}{1-g}\left(\tfrac{\beta}{\alpha} - 1\right) \\ \hat{b} &> \tfrac{1}{1-g}\left(\tfrac{1}{\alpha} - 1\right) \end{aligned}\right\} \iff \hat{b} > \frac{1}{1-g}\left(\frac{1}{\alpha} - 1\right) \tag{19}$$

For the second case (15) and (16), conditions 2 and 3 become:

$$\left.\begin{aligned} \hat{b} &> \tfrac{\hat{m}}{g}\left(\tfrac{\alpha}{\beta} - 1\right) \\ \hat{b} &> \tfrac{\hat{m}}{g}\left(\tfrac{1}{\beta} - 1\right) \end{aligned}\right\} \iff \hat{b} > \frac{\hat{m}}{g}\left(\frac{1}{\beta} - 1\right) \tag{20}$$

So, (14) is a valid non-trivial equilibrium if and only if conditions (17) and (19) hold, while (16) is a valid non-trivial equilibrium if and only if conditions (18) and (20) hold.

To consider a special case, if we assume that males and females are born and die at equal rates and that the optimal reproductive ratio of males to females in the ecosystem is one-to-one (i.e. $g = \frac{1}{2}, \alpha = \beta = \alpha_0, \hat{m} = 1$), the two equilibria coincide:

$$x^* = y^* = \frac{C}{4}\left[\alpha_0\left(2 + \hat{b}\right) - 2\right] \tag{21}$$

This is a valid non-zero equilibrium provided that it defines positive values for y^* and x^*, which is the case if and only if:

$$\hat{b} > 2\left(\frac{1}{\alpha_0} - 1\right)$$

4.3. Stability of non-trivial equilibria

Consider the Jacobian matrix J of the dynamical system (6) (following on from the previous sections, we consider only the two-dimensional dynamics of a healthy population):

$$J = \begin{pmatrix} \partial x_t/\partial x_{t-1} & \partial x_t/\partial y_{t-1} \\ \partial y_t/\partial x_{t-1} & \partial y_t/\partial y_{t-1} \end{pmatrix}$$

In this model, there are two forms for the Jacobian matrix, J_1 and J_2, for the two cases $(y_{t-1}/x_{t-1})(\beta/\alpha) \geqslant \hat{m}$ and $(y_{t-1}/x_{t-1})(\beta/\alpha) < \hat{m}$ respectively.

The stability of an equilibrium of a two-dimensional discrete-time dynamical system is determined by the eigenvalues λ_1, λ_2 of J, which may be real or complex. Without loss of generality,

suppose that $|\lambda_1| \leqslant |\lambda_2|$. A point is stable if $|\lambda_1|, |\lambda_2| < 1$ and unstable if at least one of $|\lambda_1|, |\lambda_2|$ is greater than 1.

From (6), neglecting the subscript $t-1$ for clarity, we find that:

$$\begin{aligned} \det(J_1) &= \alpha\beta\left[1+\hat{b}(1-g)\right]\left[\frac{C}{C+x+y}\right]^3 \\ \det(J_2) &= \alpha\beta\left[1+\frac{\hat{b}}{\hat{m}}g\right]\left[\frac{C}{C+x+y}\right]^3 \end{aligned} \tag{22}$$

Notice that $\det(J_1)$ and $\det(J_2)$ depend only on the total population $x+y$, and are independent of the ratio of males to females.

Substituting (14) into $\det(J_1)$ and (16) into $\det(J_2)$, we have:

$$\begin{aligned} \det(J) &= \frac{\beta}{\alpha^2}\left[1+\hat{b}(1-g)\right]^{-2} \text{ at equilibrium (14)} \\ \det(J) &= \frac{\alpha}{\beta^2}\left[1+\frac{\hat{b}}{\hat{m}}g\right]^{-2} \text{ at equilibrium (16)} \end{aligned} \tag{23}$$

For the trace, we find that:

$$\begin{aligned} \mathrm{tr}(J_1) &= C\left[\frac{\alpha(C+y)+\beta(C+x)+\alpha\hat{b}[(1-g)(C+y)-gx]}{(C+x+y)^2}\right] \\ \mathrm{tr}(J_2) &= C\left[\frac{\alpha(C+y)+\beta(C+x)+\beta\frac{\hat{b}}{\hat{m}}[g(C+x)-(1-g)y]}{(C+x+y)^2}\right] \end{aligned} \tag{24}$$

Substituting (13) and (14) into $\mathrm{tr}(J_1)$ and (15) and (16) into $\mathrm{tr}(J_2)$, we have:

$$\begin{aligned} \mathrm{tr}(J) &= \frac{\beta+1}{\alpha}\left[1+\hat{b}(1-g)\right]^{-1} \text{ at equilibrium (14)} \\ \mathrm{tr}(J) &= \frac{\alpha+1}{\beta}\left[1+\frac{\hat{b}}{\hat{m}}g\right]^{-1} \text{ at equilibrium (16)} \end{aligned} \tag{25}$$

Since $\det(J) = \lambda_1\lambda_2$ and $\mathrm{tr}(J) = \lambda_1 + \lambda_2$, we can write the eigenvalues at each equilibrium by inspection:

$$\left.\begin{aligned} \lambda_1 &= \tfrac{\beta}{\alpha}\left[1+\hat{b}(1-g)\right]^{-1}, \\ \lambda_2 &= \tfrac{1}{\alpha}\left[1+\hat{b}(1-g)\right]^{-1} \end{aligned}\right\} \text{ for equilibrium (14)}$$
$$\left.\begin{aligned} \lambda_1 &= \tfrac{\alpha}{\beta}\left[1+\tfrac{\hat{b}}{\hat{m}}g\right]^{-1}, \\ \lambda_2 &= \tfrac{1}{\beta}\left[1+\tfrac{\hat{b}}{\hat{m}}g\right]^{-1} \end{aligned}\right\} \text{ for equilibrium (16)} \tag{26}$$

Note that in each case the eigenvalues are real, positive and distinct.

Now, from (19), we see that $1+\hat{b}(1-g) > \alpha^{-1}$ at equilibrium (14). Comparing this with the expressions above shows that $|\lambda_1|, |\lambda_2| < 1$. Similarly, from (20), we see that $1+g\hat{b}/\hat{m} > \beta^{-1}$ at equilibrium (16). Again, this implies that $|\lambda_1|, |\lambda_2| < 1$.

These results guarantee the stability of non-trivial equilibria in the majority of cases. However, it remains to consider equilibria that lie on the line $y = (\alpha/\beta)\hat{m}x$ between the region in which there is an excess of males and that in which there is a deficit. Such equilibria must be shown to be stable from both sides of this interface. In other words, at an equilibrium on this line, we require that:

1. The point would be an equilibrium under both forms of B (see (5)).
2. In both cases of (26), $|\lambda_1|, |\lambda_2| < 1$ at this point.

For a non-trivial equilibrium, these conditions are easily demonstrated. Condition 1 holds through the continuity of B as function of $\tilde{x}, \tilde{y}, \tilde{z}$ on the interface. Condition 2 holds automatically for the first case of (26), since equilibrium (14) is defined on $y = (\alpha/\beta)\hat{m}x$. For the second case, from (17) and (18) we see that at an equilibrium on the boundary:

$$\hat{m} = \frac{\beta\hat{b}g}{(\alpha-\beta)+\alpha\hat{b}(1-g)}$$

Substituting this into the second case of (26), we find that

$$\lambda_1 = \left[1+\hat{b}(1-g)\right]^{-1}, \quad \lambda_2 = \frac{1}{\alpha}\left[1+\hat{b}(1-g)\right]^{-1}$$

These are both less than 1 in modulus, since we again have that $1+\hat{b}(1-g) > \alpha^{-1}$ at equilibrium (14), by (19), which confirms condition 2.

Therefore, if they exist, equilibria (14) and (16) are stable.

4.4. Stability of $(0,0)$

The point $(0,0)$ also lies on $y = (\alpha/\beta)\hat{m}x$, but since the above results were only valid for non-trivial equilibria, there is no *prima facie* guarantee that the origin will not be stable from one side of this line and unstable from the other.

By (22) and (24), at $(0,0)$, we have:

$$\begin{aligned} \det(J_1) &= \alpha\beta\left[1+\hat{b}(1-g)\right] \\ \det(J_2) &= \alpha\beta\left[1+\frac{\hat{b}}{\hat{m}}g\right] \end{aligned}$$

$$\begin{aligned} \mathrm{tr}(J_1) &= \beta+\alpha\left[1+\hat{b}(1-g)\right] \\ \mathrm{tr}(J_2) &= \alpha+\beta\left[1+\frac{\hat{b}}{\hat{m}}g\right] \end{aligned}$$

Hence by inspection, we have the following eigenvalue pairs:

$$\begin{aligned} &\lambda_1 = \beta, \ \ \lambda_2 = \alpha\left[1+\hat{b}(1-g)\right] \quad \text{for } J_1 \\ &\lambda_1 = \alpha, \ \ \lambda_2 = \beta\left[1+\frac{\hat{b}}{\hat{m}}g\right] \quad \text{for } J_2 \end{aligned} \tag{27}$$

Note that we no longer necessarily suppose that $|\lambda_1| \leqslant |\lambda_2|$.

After rearranging, sufficient stability conditions for $(0,0)$ can hence be written:

$$\hat{b} < \frac{1}{1-g}\left(\frac{1}{\alpha}-1\right) \quad \text{for the region } y \geqslant \frac{\alpha}{\beta}\hat{m}x \tag{28}$$

$$\hat{b} < \frac{\hat{m}}{g}\left(\frac{1}{\beta}-1\right) \quad \text{for the region } y < \frac{\alpha}{\beta}\hat{m}x \tag{29}$$

Note that these inequalities unsurprisingly mirror stability conditions (19) and (20) for the non-trivial equilibria. If both these conditions hold, then $(0,0)$ is stable. Otherwise, the point may be 'stable' under some perturbations but 'unstable' under others. We describe such situations as dual cases.

4.5. Analysis of dual cases

Understanding exactly what happens in the neighbourhood of $(0,0)$ for these dual cases requires further analysis of the eigenvectors of J_1 and J_2 at $(0,0)$. Clearly $[0,1]^\top$ is an eigenvector of J_1 and $[1,0]^\top$ is an eigenvector of J_2. With regard to the other eigenvectors, it is important to understand whether the gradient of each is greater than or less than the gradient $(\alpha/\beta)\hat{m}$ of the interface between regions with an excess and with a deficit of males.

The eigenvectors are:

$$\mathbf{e}_1 = \left[\frac{1}{\hat{b}g}\left(1+\hat{b}(1-g)-\frac{\beta}{\alpha}\right),1\right]^\top \quad \text{for} \quad J_1$$

$$\mathbf{e}_2 = \left[1,\frac{\hat{m}}{\hat{b}(1-g)}\left(1+\frac{\hat{b}}{\hat{m}}g-\frac{\alpha}{\beta}\right)\right]^\top \quad \text{for} \quad J_2$$

Note that the first component of $\mathbf{e}_1$ and the second component of $\mathbf{e}_2$ may be equal to zero, leading to degenerate behaviour. We disregard these situations, since they are not preserved under small perturbations of the parameters and are therefore unlikely to occur in reality.

Suppose that, according to our analysis, $(0,0)$ is potentially 'unstable' in the region $y \geqslant (\alpha/\beta)\hat{m}x$ in which there is an excess of males, and 'stable' in the region $y < (\alpha/\beta)\hat{m}x$ in which there is a deficit of males. This means that (29) holds and (28) does not hold:

$$\hat{b} \geqslant \frac{1}{1-g}\left(\frac{1}{\alpha}-1\right) \tag{30}$$

$$\hat{b} < \frac{\hat{m}}{g}\left(\frac{1}{\beta}-1\right) \tag{31}$$

Clearly, the gradient of $\mathbf{e}_1$, the eigenvector associated with the 'unstable' region, is not equal to zero. We also observe that it cannot be negative, since this would imply:

$$\hat{b} < \frac{1}{1-g}\left(\frac{\beta}{\alpha}-1\right) < \frac{1}{1-g}\left(\frac{1}{\alpha}-1\right)$$

which contradicts (30).

Now assume that the gradient of $\mathbf{e}_1$ is greater than or equal to the gradient of the interface:

$$\hat{b}g\left(1+\hat{b}(1-g)-\frac{\beta}{\alpha}\right)^{-1} \geqslant \frac{\alpha}{\beta}\hat{m}$$

Having established that the gradient is non-negative, this can be rearranged as:

$$\hat{b} \geqslant \frac{\hat{m}}{g}\left[\frac{\alpha}{\beta}\left(1+\hat{b}(1-g)\right)-1\right] \tag{32}$$

and, by (30), this implies:

$$\hat{b} \geqslant \frac{\hat{m}}{g}\left[\frac{\alpha}{\beta}\left(1+\frac{1}{1-g}\left(\frac{1}{\alpha}-1\right)(1-g)\right)-1\right]$$

$$\Rightarrow \hat{b} \geqslant \frac{\hat{m}}{g}\left(\frac{1}{\beta}-1\right) \tag{33}$$

which contradicts (31). Hence, the assumption was false and the gradient of $\mathbf{e}_1$ must be less than the gradient of the interface and greater than zero.

Now assume that the gradient of $\mathbf{e}_2$ is greater than or equal to the gradient of the interface:

$$\frac{\hat{m}}{\hat{b}(1-g)}\left(1+\frac{\hat{b}}{\hat{m}}g-\frac{\alpha}{\beta}\right) \geqslant \frac{\alpha}{\beta}\hat{m}$$

This can be rearranged as:

$$\hat{b} \leqslant \frac{1}{1-g}\left[\frac{\beta}{\alpha}\left(1+\frac{\hat{b}}{\hat{m}}g\right)-1\right] \tag{34}$$

and, by (31), this implies:

$$\hat{b} < \frac{1}{1-g}\left[\frac{\beta}{\alpha}\left(1+\frac{\hat{m}}{g}\left(\frac{1}{\beta}-1\right)\frac{g}{\hat{m}}\right)-1\right] \Rightarrow \hat{b} < \frac{1}{1-g}\left(\frac{1}{\alpha}-1\right) \tag{35}$$

which contradicts (30). Hence, the gradient of $\mathbf{e}_2$ must be less than the gradient of the interface, becoming non-positive when:

$$\hat{b} \leqslant \frac{\hat{m}}{g}\left(\frac{\alpha}{\beta}-1\right) \tag{36}$$

So, if $(0,0)$ is potentially 'unstable' in the region $y \geqslant (\alpha/\beta)\hat{m}x$ and 'stable' in the region $y < (\alpha/\beta)\hat{m}x$, as we supposed, then we have shown that, when the eigenvectors are anchored at $(0,0)$, neither is directed into the region above the interface, with $\mathbf{e}_1$ directed between the interface and the x-axis and $\mathbf{e}_2$ directed into the same region or into the negative quadrant. The two possible classes of dynamical behaviour are illustrated in Fig. 2. Trajectories are represented as curves for ease of understanding, though they are actually sequences of discrete points.

The key point is that the eigenvector $\mathbf{e}_1$ associated with unstable behaviour is not directed into the region in which this instability occurs. Therefore, near $(0,0)$, trajectories from this 'unstable' region must cross the interface and then converge to $(0,0)$ along a path which becomes parallel to $\mathbf{e}_2$ if this vector is directed into the positive quadrant (Fig. 2 (**i**)), or to the x-axis if it is not (Fig. 2 (**ii**)). To see that $\mathbf{e}_2$ dominates the behaviour of trajectories near $(0,0)$ in situation **(i)** while $[1,0]^\top$ dominates the behaviour of trajectories near $(0,0)$ in situation **(ii)**, it suffices to consider the relative size of the eigenvalues of J_2 when (36) is true and when it is false.

A similar argument can be made to demonstrate that the two eigenvectors have gradient greater than that of the interface when $(0,0)$ is 'stable' in the region $y \geqslant (\alpha/\beta)\hat{m}x$ and potentially 'unstable' in the region $y < (\alpha/\beta)\hat{m}x$.

There remains an ambiguous case in which neither (28) nor (29) holds, but where:

$$\hat{b} = \max\left[\frac{1}{1-g}\left(\frac{1}{\alpha}-1\right),\frac{\hat{m}}{g}\left(\frac{1}{\beta}-1\right)\right]$$

In this case, the point $(0,0)$ is stable, since the relevant equations that should define a stable non-trivial equilibrium, (14) or (16), can be shown to coincide with the origin.

Hence, $(0,0)$ is unstable if and only if:

$$\hat{b} > \max\left[\frac{1}{1-g}\left(\frac{1}{\alpha}-1\right),\frac{\hat{m}}{g}\left(\frac{1}{\beta}-1\right)\right]$$

4.6. Parameter variation

(14) and (16) and their accompanying existence conditions, constitute an explicit description of the non-trivial spatially uniform equilibria of the model. In Section 5 we attempt to determine realistic values for the parameters, but it should be noted that alongside the 'fast' population dynamics described by the model the parameters may also change on longer time scales. In particular, the number of mosquitoes that ultimately reach adulthood from a single oviposition depends on temperature and rainfall, leading to significant seasonal variations in the population [9]. In our model, this variation is contained in the parameter $\hat{b}$, so it is sensible to examine how the dynamics change as $\hat{b}$ varies.

Eliminating $\hat{b}$ from (14) provides the locus of the equilibrium in the region $y \geqslant (\alpha/\beta)\hat{m}x$:

$$x^2 - Gy^2 + (1-g)xy + (1-\alpha)Cx - (1-\beta)CGy = 0 \tag{37}$$

where

$$G = \frac{1}{g} - 1$$

Eliminating $\hat{b}$ from (16) yields the same equation. This indicates that for fixed values of g, α and β, the potential equilibria for populations with an excess of males and for those with a deficit lie on the same curve in the phase plane. Choosing a particular value of $\hat{b}$ determines the position of each of the potential equilibria on this curve. From Section 4.2, we know that at most one of these points will lie in the region of the phase plane in which it defines a true equilibrium.

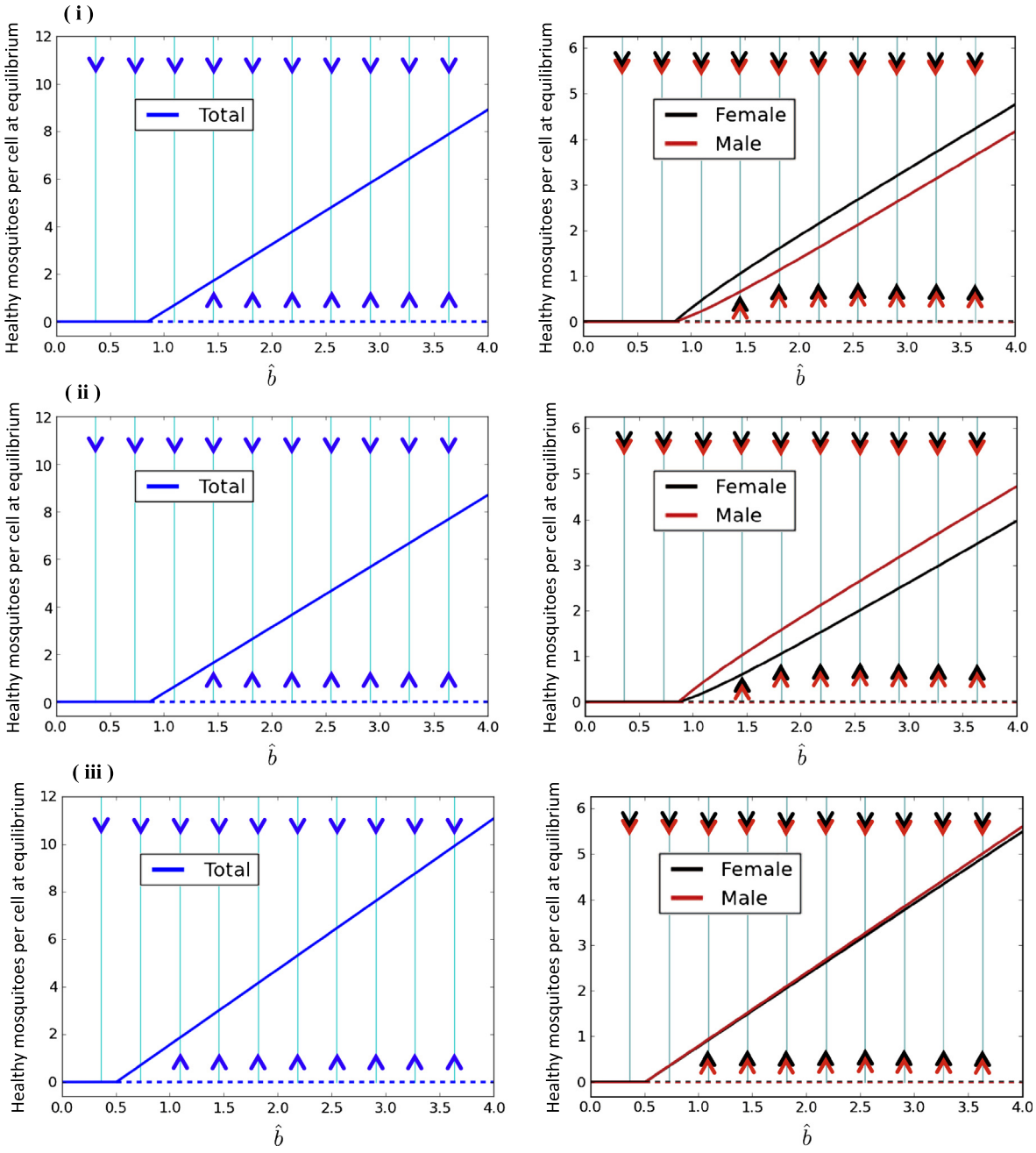

Fig. 3. Bifurcation diagrams for the spatially uniform equilibria of the healthy population as $\hat{b}$ varies. Solid graph lines represent stable equilibria, while dotted graph lines represent unstable equilibria. Arrowheads indicate convergence to equilibrium for different values of $\hat{b}$. The parameters for each subfigure are: **(i)** $\alpha = \frac{9}{10}, \beta = \frac{7}{10}, C = 8, g = \frac{51}{101}, \hat{m} = 1$ [Deficit of males at (x^*, y^*)] **(ii)** $\alpha = \frac{7}{10}, \beta = \frac{9}{10}, C = 8, g = \frac{51}{101}, \hat{m} = 1$ [Excess of males at (x^*, y^*)] **(iii)** $\alpha = \frac{8}{10}, \beta = \frac{8}{10}, C = 8, g = \frac{51}{101}, \hat{m} = \frac{51}{50}$ ['Optimal' gender ratio at (x^*, y^*)] where (x^*, y^*) represents the non-trivial equilibrium, where it exists.

Eq. (37) defines a conic, whose squared eccentricity is given by:

$$e^2 = 2\sqrt{2}\left[\frac{\sqrt{G^2+1}}{\sqrt{2}\sqrt{G^2+1} \pm (1-g)}\right] \tag{38}$$

where the sign of $(1-g)$ in the denominator matches the sign of $(\alpha - \beta)$.

Observe that, in both cases, the right hand side of (38) is greater than $1, \forall g > 0$, and therefore, since the eccentricity is a non-negative quantity, we have that $e \in (1, \infty), \forall g > 0$. Therefore, the locus of the equilibrium as $\hat{b}$ varies is part of a (possibly degenerate) hyperbola for all values of the other parameters.

One question that can be posed about the system is whether the population of mosquitoes can pass from an equilibrium state in which there is a deficit of males to one in which there is an excess as $\hat{b}$ varies. This situation can occur if Eq. (37) and the interface $y = (\alpha/\beta)\hat{m}x$ intersect at some point with positive x and y coordinates. Aside from the origin, the intersection point is given by:

$$\begin{aligned} x &= \beta C\left[\frac{(1-\alpha)\beta - \alpha(1-\beta)G\hat{m}}{(\alpha\hat{m}+\beta)(\alpha\hat{m}G-\beta)}\right] \\ y &= \alpha C\hat{m}\left[\frac{(1-\alpha)\beta - \alpha(1-\beta)G\hat{m}}{(\alpha\hat{m}+\beta)(\alpha\hat{m}G-\beta)}\right] \end{aligned} \tag{39}$$

and it is easy to check whether or not these equations define positive x and y values for a given set of parameters.

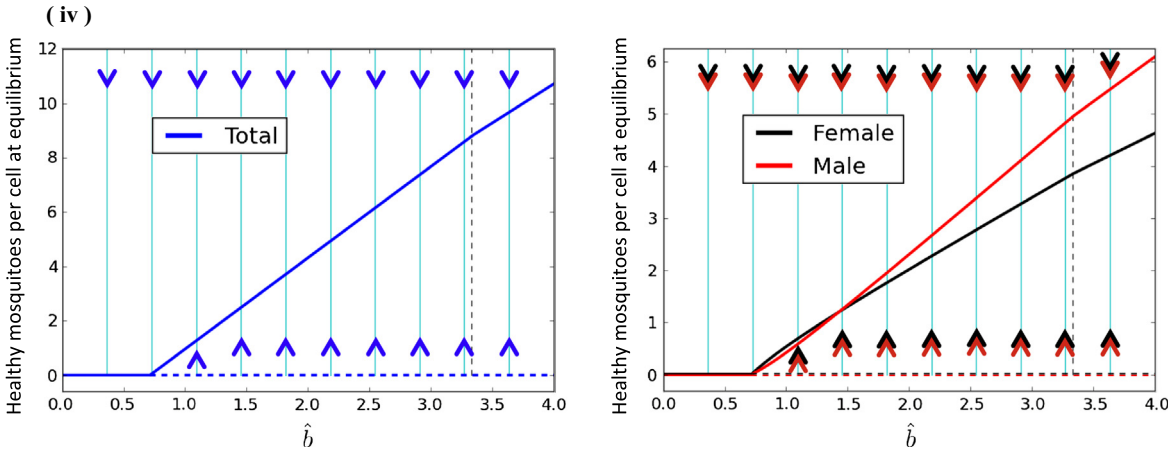

Fig. 4. Bifurcation diagrams for the spatially uniform equilibria of the healthy population as $\hat{b}$ varies. Solid graph lines represent stable equilibria, while dotted graph lines represent unstable equilibria. Arrowheads indicate convergence to equilibrium for different values of $\hat{b}$. The parameters for this subfigure are: **(iv)** $\alpha = \frac{9}{10}, \beta = \frac{7}{10}, C = 8, g = \frac{3}{5}, \hat{m} = 1$. In this case, whether there is a deficit or an excess of males at the non-trivial equilibrium (x^*, y^*) depends on $\hat{b}$. The vertical dotted line indicates the point at which (x^*, y^*) crosses the interface $y = (\alpha/\beta)\hat{m}x$ from the zone in which there is a deficit to the zone in which there is an excess.

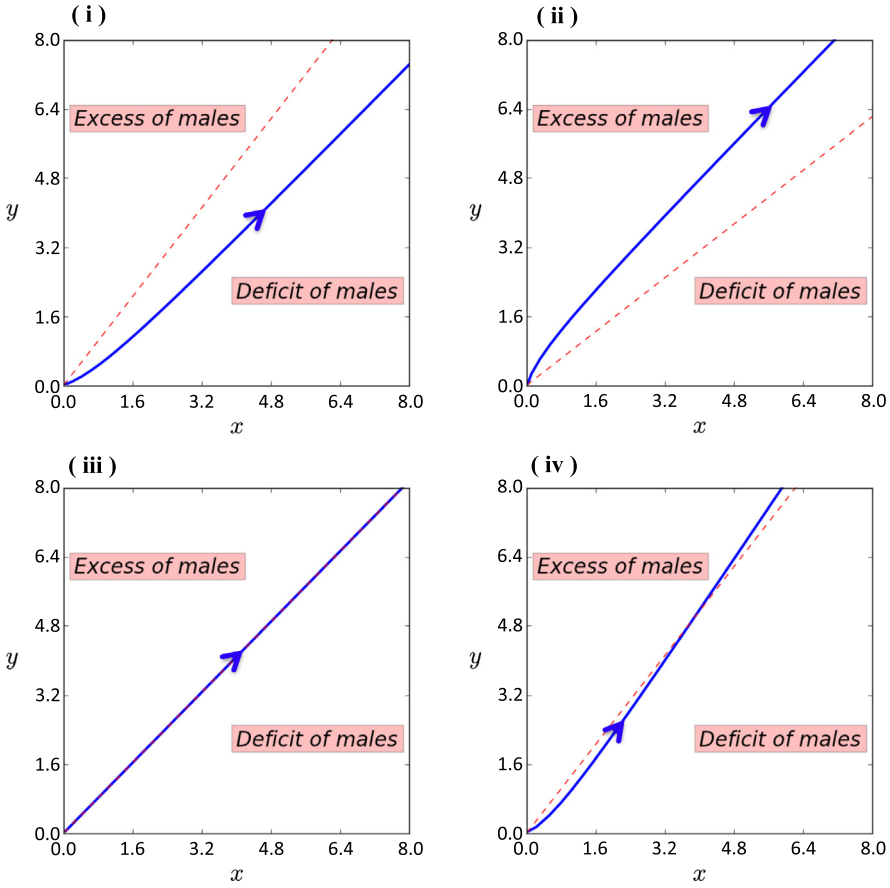

Fig. 5. The locus of the non-trivial equilibrium (x^*, y^*) as $\hat{b}$ varies. The arrows indicate the direction of increasing $\hat{b}$. The interface $y = (\alpha/\beta)\hat{m}x$ between zones with an excess and with a deficit of males is indicated with a dotted line. The parameters for each subfigure are: **(i)** $\alpha = \frac{9}{10}, \beta = \frac{7}{10}, C = 8, g = \frac{51}{101}, \hat{m} = 1$ [Deficit of males at (x^*, y^*)] **(ii)** $\alpha = \frac{7}{10}, \beta = \frac{9}{10}, C = 8, g = \frac{51}{101}, \hat{m} = 1$ [Excess of males at (x^*, y^*)] **(iii)** $\alpha = \frac{8}{10}, \beta = \frac{8}{10}, C = 8, g = \frac{51}{101}, \hat{m} = \frac{51}{50}$ ['Optimal' gender ratio at (x^*, y^*)] **(iv)** $\alpha = \frac{9}{10}, \beta = \frac{7}{10}, C = 8, g = \frac{3}{5}, \hat{m} = 1$ [Deficit, excess and 'optimal' cases all possible, depending on $\hat{b}$]

Note that in the special case where $\alpha\hat{m}G = \beta$, there are two possible situations:

- If $\alpha \neq \beta$, then the origin is the only point of intersection.
- If $\alpha = \beta$, then (37) and $y = (\alpha/\beta)\hat{m}x$ coincide. In this case, if the non-trivial equilibrium exists then it necessarily has the 'optimal' ratio $\hat{m}$ of males to females.

The changing behaviour of the system as $\hat{b}$ is varied is visualised in Figs. 3–6. Figs. 3 and 4 show bifurcation diagrams of the dynamics of the healthy population as $\hat{b}$ varies for four distinct cases, clearly indicating the bifurcation described in Section 3.6. Fig. 5 shows the locus of the non-trivial equilibrium (x^*, y^*) as $\hat{b}$ varies for the same four cases. Fig. 6 presents vector fields of the dynamics and the location of (x^*, y^*) for particular values of $\hat{b}$.

5. Parametrisation of the model for *Aedes aegypti*

5.1. Objectives

In this section, with reference to previous research, we attempt to determine sensible values for the parameters $p, \alpha, \beta, \gamma, \hat{b}, g, \hat{m}, r, \nu$ and C, and for the cell-size and time increment, such that the model may represent the dynamics of an SIT programme for *Aedes aegypti*. We also attempt to determine what a sustainable overall rate of sterile insect release for such a programme might be.

Naturally, the values chosen should in no way be seen as definitive, not least because most would be expected to vary considerably, both geographically and seasonally, or to depend on the precise way in which sterile insects are produced. They should rather be seen as reasonable initial values for our simulations, through which a broad analysis of the behaviour of the model may be performed.

A summary of the final values chosen for each parameter, along with the sources from which they were derived, is provided by Table 1.

5.2. Dispersal

Shelly and McInnis [2] argue that any successful SIT programme for *Aedes aegypti* "demands a very fine spatial scale" owing to the low dispersal rate of the insect. Estimates of the mean distance travelled per day by *Aedes aegypti* vary considerably between studies. Muir and Kay [46] calculated values of 24.7 m and 18.2 m for females and males released outdoors, and commented that dispersal rates "would depend on the physical characteristics of the study site ...and on the physiological state of the mosquitoes." Sheppard et al. [47] estimated a mean distance travelled per day of 37 metres.

A mark–release–recapture study of the dispersal of the species in Cairns, Australia [48] divided the recapture zone into annuli whose radii increased by increments of 50 m. If we similarly set the distance between the centres of neighbouring cells in our model to 50 m, the time increment of the model to 24 h and the value $p = 0.4$, the mean distance travelled by mosquitoes in a single time increment (one day) is $50(1 - 0.4) = 30$ m, which is of a similar order to the estimates cited.

Table 1
Summary of parameter values used in the model simulations and the sources from which they were derived. Note that the values are not necessarily drawn directly from the sources; rather, where multiple sources are cited, they have been compared and combined to deduce reasonable values for the relevant parameter. Discussion of the reasoning behind these decisions can be found in the given sections of the text.

Parameter	Value used in simulations	Sources	See Section...
p	0.4	[2,46,47]	5.2
α	0.9	[9,46,49]	5.3
β	0.7	[9,46,49]	5.3
γ	0.6	*See text.*	5.3
$\hat{b}$	16	[9,46]	5.4
g	51/101	[50]	5.4
$\hat{m}$	1	*See text.*	5.4
r	0.56	[5]	5.4
ν	0.035	[5]	5.4
C	8	[9,51,52]	5.5
Distance between centres of neighbouring cells represents...	50 m	[48]	5.2
One model iteration represents...	24 h	*See text.*	5.2

5.3. Mortality

Most models and studies of *Aedes aegypti* dynamics agree on a survival rate per day of around 0.9 for healthy female mosquitoes, though the value decreases with the age of the insect [9,46,49]. For males there is more variation in the figure used, with estimates ranging between 0.53 and 0.87. We take the values $\alpha = 0.9$, $\beta = 0.7$. Since there are many variations of SIT, with transgenic methods developing all the time, choosing a realistic survival rate for sterile males in a hypothetical future control programme is difficult. We assume that the 'sterilisation' procedure decreases the survival rate slightly and set $\gamma = 0.6$.

5.4. Reproduction

Female *Aedes aegypti* lay an average of 63 eggs in a single gonotrophic cycle [9]. A gonotrophic cycle lasts around four days [46], though a female's first cycle is shorter than normal [9]. We take a value of $\hat{b} = 16$, the average number of healthy offspring per female per day, assuming that there is no deficit of males. This may be an overestimate, since a significant proportion of eggs will fail to develop into sexually mature adults (see [24]).

Arrivillaga and Barrera [50] found that the ratio of males to females that reach maturity (as opposed to the gender ratio of mosquitoes living in the environment) is 1.02, which suggests a value of $\frac{51}{101}$ for g. The correct value of $\hat{m}$, the minimal ratio of males to females in the environment such that females can reproduce at their maximum rate, is unknown. For our simulations, we take $\hat{m} = 1$.

A recent study by Harris et al. [5] found that the relative reproductive fitness of genetically modified males for SIT was 0.56. The same study showed that 3.5% of the offspring of these males were viable when mating with healthy females. This suggests parameter values of $r = 0.56, \nu = 0.035$.

5.5. Population density

Although C was defined in terms of the effect of overcrowding on insect mortality, it effectively governs the density of the healthy mosquito population at equilibrium, as seen in (7) and (8). Since mosquito density varies according to the terrain and the temperature and displays seasonal cycles [9,17], it is impossible to choose a value for C that would be appropriate in all circumstances.

A comparison of the conclusions of the following studies illustrates the extent of this variation. A 1960–1961 study of *Aedes aegypti* in Pensacola, Florida [51] estimated an indigenous population of approximately 3.56 male mosquitoes per hectare in a suburban area of 238 acres (96 hectares) in July 1960, and of approximately 67.9 male mosquitoes per hectare in a rural area of 48 acres (19 hectares) in July 1961. In contrast, a 1970 study carried out over a scrap heap in Dar-es-Salaam, Tanzania [52] produced estimated female populations of around 2300 per hectare on 19 September, dropping to just over 900 per hectare a little over a month later. More recently, a simulation of *Aedes aegypti* populations in Buenos Aires, Argentina [9] indicated population cycles of between 0 and 400 adult mosquitoes per hectare across the year.

Given the values chosen for the other parameters, using the results of Section 3.6, our model predicts an equilibrium population density of $5.36C$ healthy mosquitoes per cell, which corresponds to $24.7C$ healthy mosquitoes per hectare (to 3 significant figures). For the purposes of the simulation, we set $C = 8$, resulting in an equilibrium population density of approximately 197.9 healthy mosquitoes per hectare, very broadly in line with the widely spread observed and simulated population densities discussed above.

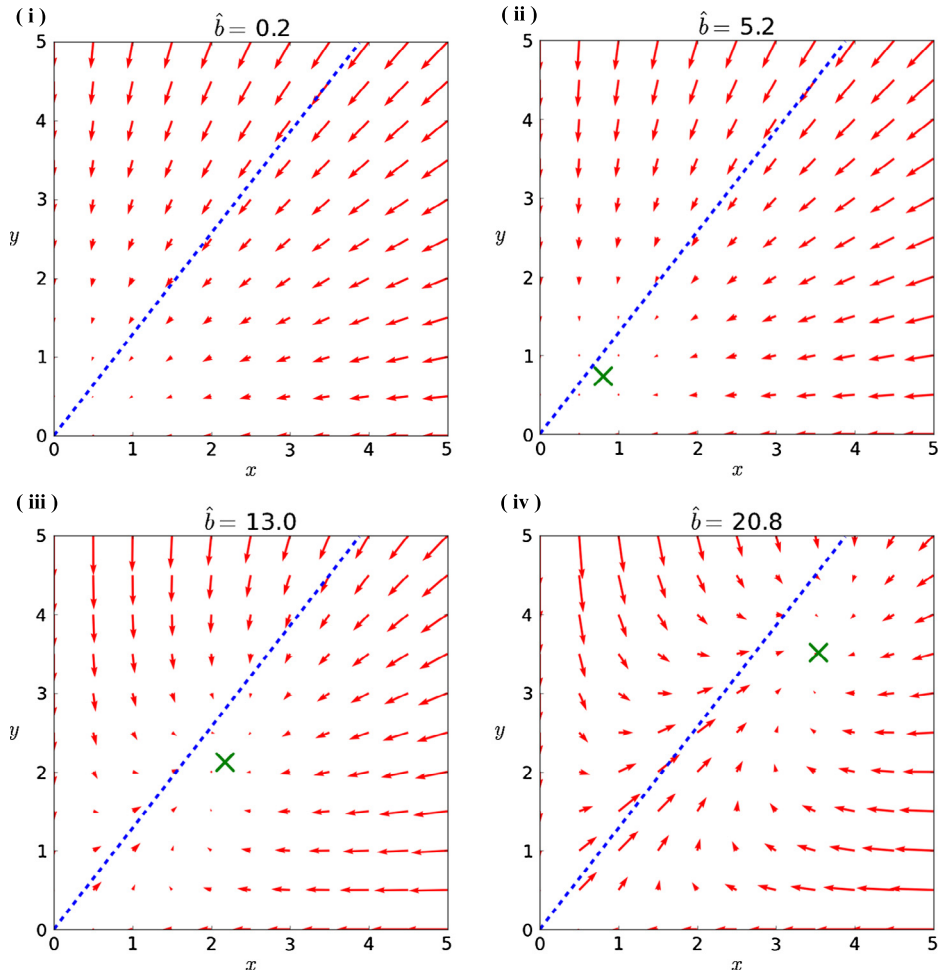

Fig. 6. Dynamics of the healthy population for varying values of $\hat{b}$ with $\alpha = \frac{9}{10}, \beta = \frac{7}{10}, C = 1, g = \frac{51}{101}, \hat{m} = 1$. The cross indicates the non-trivial equilibrium (x^*, y^*), where it exists. The interface $y = (\alpha/\beta)\hat{m}x$ between zones with an excess and with a deficit of males is indicated with a dotted line.

5.6. Volume of sterile male releases

To gain an insight into the volume of sterile male releases that may be sustainable, the aforementioned 1960–1961 Pensacola SIT study involved a mean release rate of over 100 000 sterile males per week (4 600 000 sterile male releases over 43 weeks [3]). Indeed, much higher volumes may be possible and have been achieved with other species, such as in the successful programme to control screwworm fly (*Cochliomya omnivorax*) in 1958, also in Florida, in which around 50 000 000 flies were released per week over a period of eighteen months [32]. [1] note that "the largest single sterile-insect production facility in the world produces around 2 billion sterile male Medflies per week", while certain mosquito species have reared at volumes of greater than 1 000 000 males per day.

6. Analysis of release strategies for SIT

6.1. Simulation methodology

A computer simulation of the model was used to examine the impact of three factors on the effectiveness of SIT in reducing *Aedes aegypti* populations: the number of release sites, the interval between pulsed releases and the overall mean volume of sterile mosquitoes released per unit of time.

Simulations were performed over a lattice of 144 hexagonal cells, arranged in 12 rows of 12. To eliminate edge effects, opposite edges of the grid were considered to be connected such that, in Fig. 7, all cells marked 'B' are neighbours of 'A' and all cells marked 'D' are neighbours of 'C'. To interpret the use of periodic spatial boundary conditions of this sort, we suppose that an SIT programme is applied 'evenly' to a large region of which the simulation zone represents a smaller part. The validity of the use of

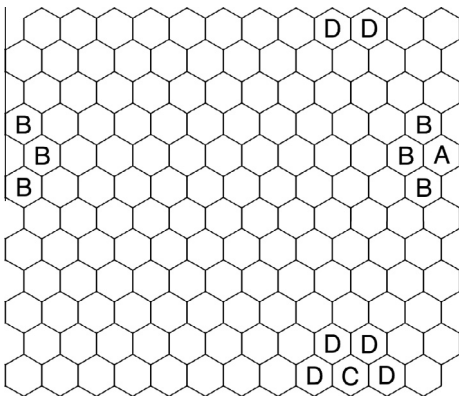

Fig. 7. The simulation zone

periodic boundary conditions to model large spatial regions in this way has been investigated (and confirmed) by [53].

Based on our parameters, the simulation zone has an area of approximately 312 000 square metres (31.2 hectares) and is roughly rectangular, measuring 600 m by 520 m. In applications of the model, the size and shape of the region and the nature of the boundaries would naturally depend on the area to be represented.

In all runs of the simulation, in common with the approach of Yakob and Bonsall [34] to model SIT control of an established wild mosquito population, the initial population of healthy males and healthy females was set at the spatially uniform equilibrium determined in Section 3.6: approximately 99.7 healthy females and 98.1 healthy males per hectare, corresponding to 21.6 healthy females and 21.2 healthy males per cell (all to 3 significant figures). Naturally, the model is sufficiently flexible that other initial distributions of mosquitoes could be simulated to match field observations for a specific location.

6.2. Sample runs

Figs. 8 and 9 show the results of 20 sample runs of the simulation for various release intervals and numbers of release sites. For each run, sterile insect releases commenced at the eighth iteration (i.e. after one week). A random spatial release strategy was employed, similar to that of Ferreira et al. [4], such that for each individual pulsed release, an appropriate random sample of the 144 cells was chosen as the release sites and available sterile male mosquitoes were divided evenly between these cells. A brief discussion of alternative patterns of sterile insect releases can be found in the appendix.

In each case, the total number of insects released was fixed to ensure a mean release rate of 100 000 sterile males per week (7 iterations) across the entire simulation zone. This corresponds to a mean rate of release of approximately 3200 sterile males per hectare per week. Recall that for the sake of simplicity, the model does not require that insect populations per cell be integers.

The 20 runs depicted in Figs. 8 and 9 were chosen as representative examples of the much larger number of simulations that were conducted. They illustrate several key features of the population dynamics, which were widely observed across all runs of the model.

Firstly, in all cases, the greater the number of sites over which sterile males are divided, the more effective the release strategy seems to be in reducing the size of the healthy population. Similarly, though the mean rate of release is the same in all cases, shorter intervals between pulsed releases seem to be more

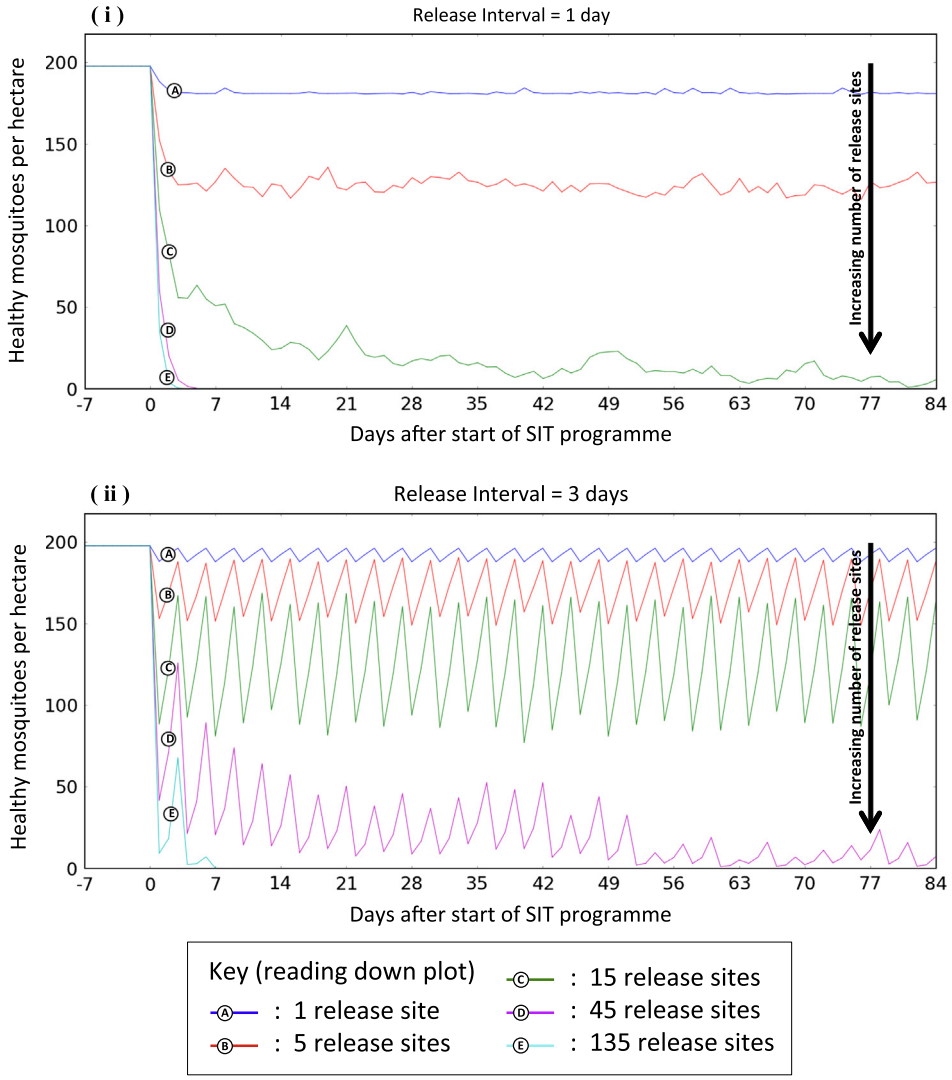

Fig. 8. Sample simulations of the effect of SIT on a wild mosquito population for varying release intervals and numbers of release sites. Reading down each plot, graphs relate to increasing numbers of release sites, as seen in the key.

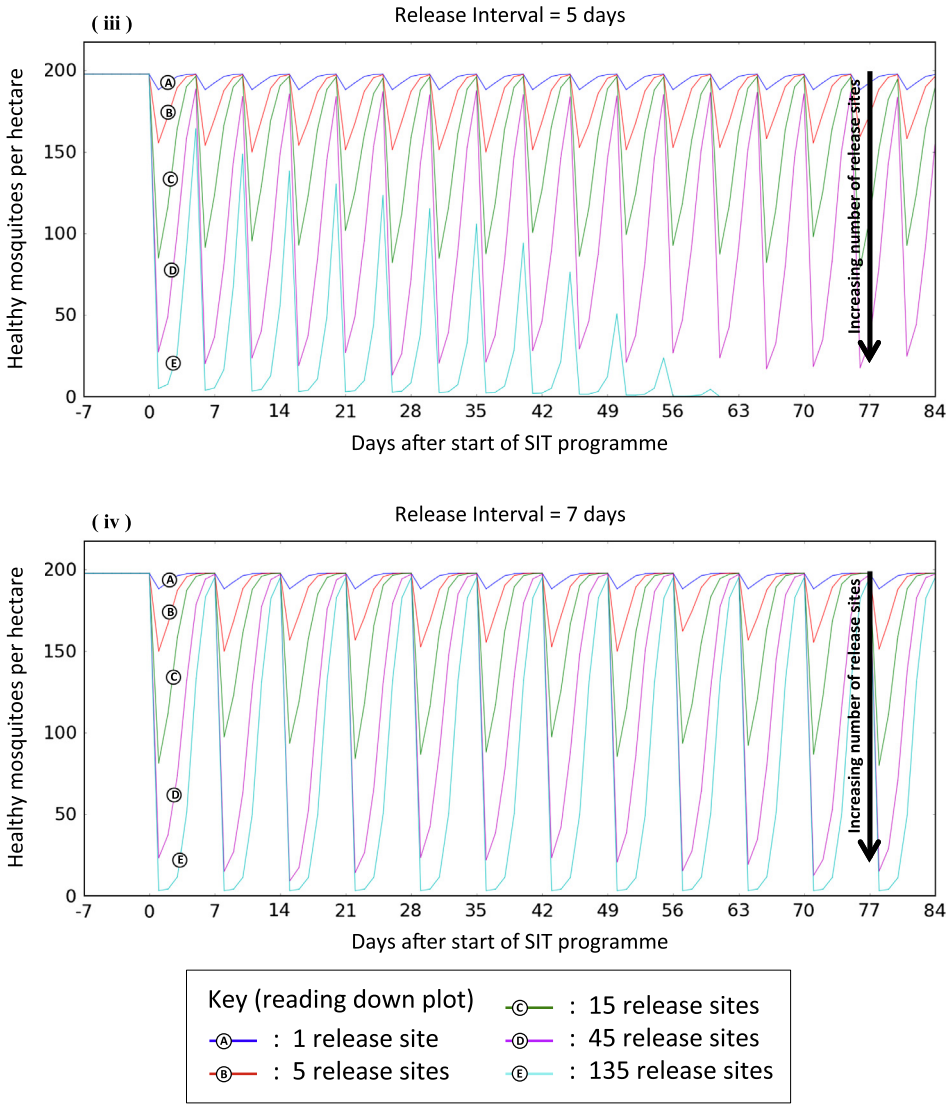

Fig. 9. Sample simulations of the effect of SIT on a wild mosquito population for varying release intervals and numbers of release sites. Reading down each plot, graphs relate to increasing numbers of release sites, as seen in the key.

effective than greater intervals, in line with the findings of White et al. [40], Dumont and Tchuenche [41], and Dufourd and Dumont [42,43].

Secondly, it is evident from the figures that while sterile male releases can dramatically reduce the size of the healthy population in the short term, recovery between releases is extremely rapid. For the greater release intervals seen in Fig. 9, it can be seen that even when reduced to extremely low levels by widely spatially spread releases, the healthy population is able to bounce back quickly, such that in many cases the population has recovered almost to the healthy equilibrium before the next releases take place.

Examining individual runs suggests that this may be due not only to a rapid rate of convergence to equilibrium in the model, but also to the fact that since sterile males are released in dense groups, they are subject to high mortality. This results in a low dispersal of sterile males and the persistence of pockets of healthy mosquitoes that are largely unaffected by sterile releases and are therefore able to rapidly recolonise those areas in which healthy insects have been wiped out.

This finding is in line with the observations of several other authors [16,17,29,34] regarding local eradication and recolonisation processes in SIT models. However, it has a potentially interesting implication for the design of SIT programmes that has apparently not been noted in previous work, since few authors have explicitly considered the spatial distribution of sterile insect release sites in pulsed release models.

Specifically, this finding suggests that it may be necessary to carefully consider any density dependent mortality of sterile males, their rate of dispersal and the density of the wild population to determine the optimal distance between release sites, interval between pulsed releases and number of sterile males released together at each location, to ensure that the number of unnecessary deaths of sterile males due to localised high population densities is minimised. If this effect truly exists in real world applications of SIT, failure to take these factors into account could lead to costly and ineffective control programmes.

Thirdly, for those sample runs with release intervals greater than 1 day, two distinct dynamical behaviours are evident. Either the healthy population is eradicated or it settles into fairly regular oscillations whose period is equal to the release interval. The main exception is the run representing a release strategy of 45 release sites, with a release interval of 3 days, where it is not clear from Fig. 8(ii) whether the long term dynamics will conform to one of

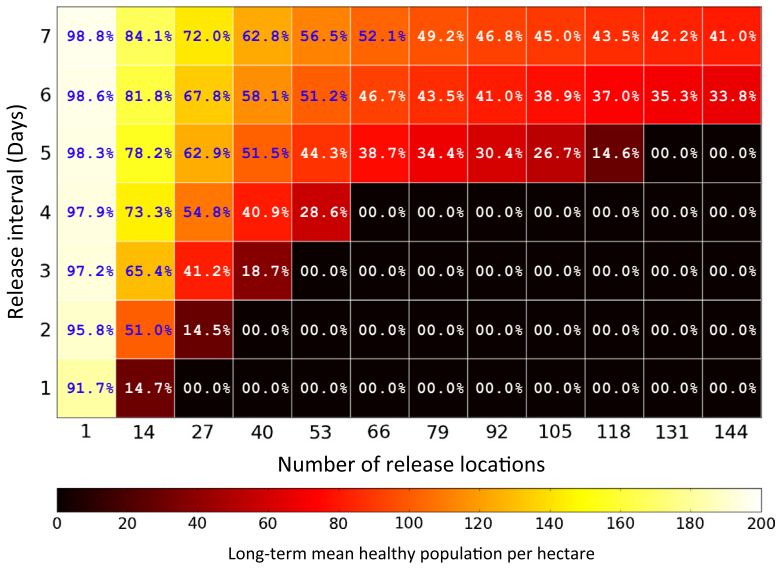

Fig. 10. The effect of SIT on the healthy population for 84 different release strategies. Percentages indicate the size of the healthy population, averaged across the final 120 iterations (119 iterations for release intervals of 7 days) of each of 10 simulations of 300 iterations, relative to the equilibrium value of approximately 197.9 insects per hectare.

these two types or display some form of irregular oscillatory behaviour.

Of the 5 sample runs with release intervals of 1 day, in those for 1 and 5 release sites, the healthy population seems to settle to a noisy equilibrium, for 45 and 135 release sites the healthy population is rapidly eradicated, while for 15 release sites, it is again unclear from Fig. 8(i) whether the long term dynamics will conform to one of these two types or display some form of irregular oscillatory behaviour.

6.3. Release interval and number of release sites

To examine the effect of varying the release interval and number of release sites in more detail, 84 different release strategies were considered, with the release interval ranging from 1 to 7 days and the number of sites ranging from 1 to 144 (the latter representing a uniform release of sterile males in every cell).

To measure the success of a particular release strategy, the simulation was run for 300 iterations and the mean size of the healthy population per hectare was calculated over the final 120 iterations for release intervals of 1 to 6 days or the final 119 iterations for a release interval of 7 days (ensuring that a whole number of release cycles was included in each calculation). The mean of these values was calculated over 10 runs to obtain a measure of the long-term mean healthy population per hectare for each release strategy. As in Section 6.2, releases commenced at the eighth iteration, were divided evenly between randomly chosen release sites and the overall rate of sterile male production was fixed at 100 000 insects per week.

The results are presented in Fig. 10. The percentages in the figure compare the observed long-term mean healthy population per hectare from the simulations to the healthy equilibrium of 197.9 insects per hectare. It should be noted that, while percentages of 0% indicate eradication, the non-zero percentages mostly do not represent stable states, but the averages of high-amplitude oscillations, as seen in Figs. 8 and 9.

The figure supports the hypothesis that lower release intervals and higher numbers of release locations are more effective in reducing the size of the healthy population. It can also be observed that for release intervals of 5 days or more, the value of increasing the number of release locations is significantly reduced. For release intervals of 6 or 7 days, even distributing sterile males evenly across every cell is not sufficient to reduce the healthy population to below a third of its equilibrium value on average. This suggests that there may be some threshold release interval (4 days in this model and with these parameters), above which the efficiency of a release strategy is seriously compromised.

It should also be noted that Fig. 10 shows that even for daily releases, more than 14 release sites were required across the simulation region to induce eradication of the healthy population, corresponding to greater than 2.2 release sites per hectare, thus supporting the assertion of Shelly and McInnis [2] that a successful SIT programme for *Aedes aegypti* demands "a very fine spatial scale".

6.4. Release volume

Using a similar method to that of Section 6.3, further runs were performed in which the overall rate of sterile male production in the model was varied between 10^1 and 10^7 individuals per week.

Since the parameter values determined in Section 5 are necessarily rather broad estimates, it would be unreasonable to draw conclusions from the model that rely strongly on absolute numbers of insects. The structure of the dynamical Eqs. (6), which are invariant under the multiplication of the variables $x_{i,t}, y_{i,t}, z_{i,t}$ by a common factor, suggests that some consideration of the relative sizes of the populations would be a more justifiable approach.

For this reason, rather than considering absolute volumes of sterile male releases, we instead consider the ratio of the overall rate of sterile male production per week to the equilibrium population of healthy males across the entire simulation zone (approximately 3060). In Fig. 11, which shows the long-term mean healthy populations per hectare calculated from simulations for various SIT strategies, this quantity is referred to as the "production ratio per unit area" and is plotted on a logarithmic scale. As before, each point plotted represents an average across 10 runs, over the final 119 or 120 of 300 iterations.

The production ratio is a convenient measure of the intensity of sterile male releases both because it is simple to convert between it and the absolute volume of sterile males produced in the model

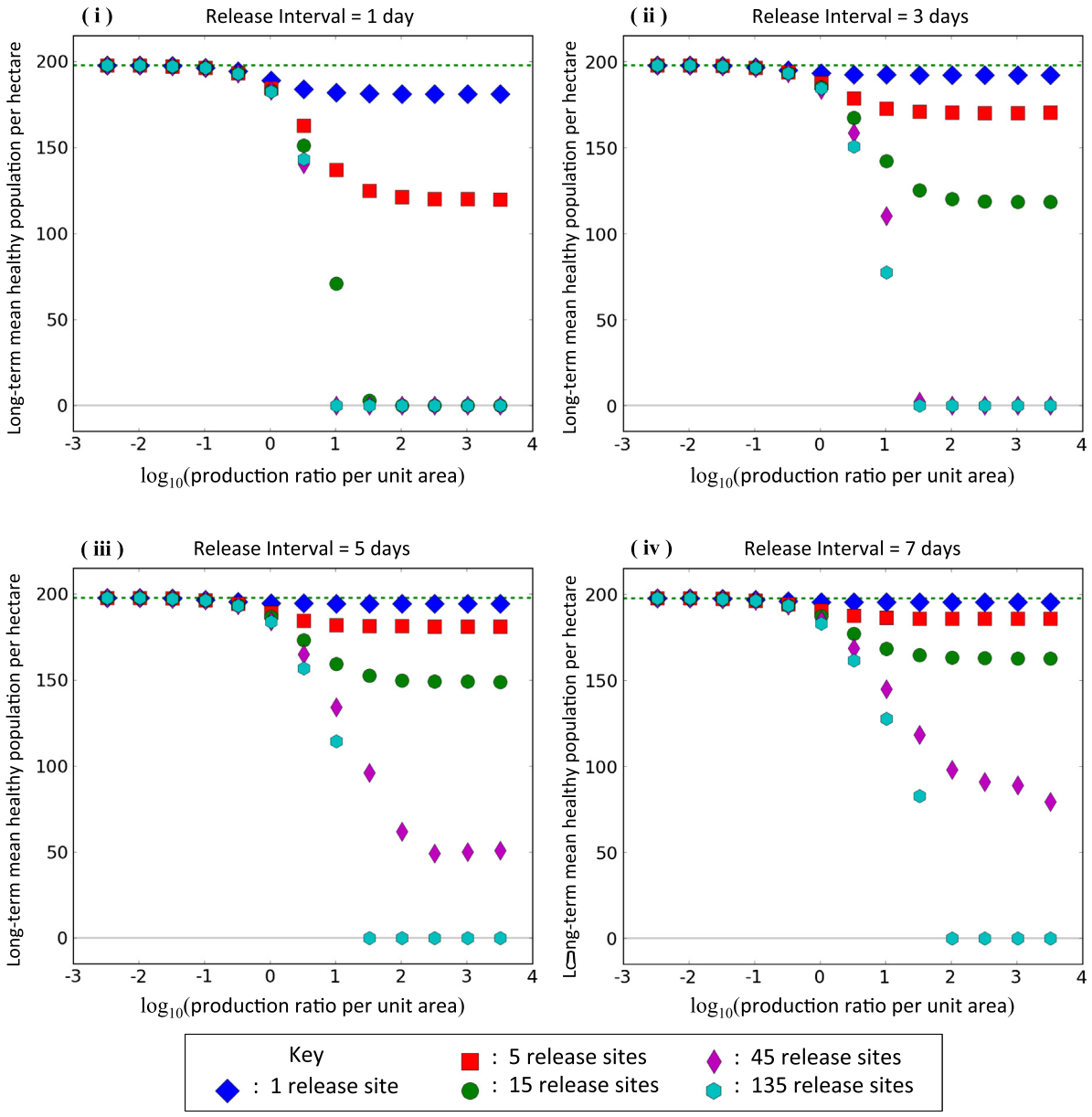

Fig. 11. The effect of varying sterile insect production on the long-term size of the healthy population. The dotted line indicates the equilibrium healthy population of approximately 197.9 insects (of both genders) per hectare. Production ratio per unit area is the ratio of overall sterile male production per week to the equilibrium population of healthy males.

(a production ratio of 10^k is approximately equal to a model weekly production of $10^{k+3.5}$ sterile males) and because it facilitates comparison with other works that also consider ratios of sterile to healthy males (e.g. [29,34,36]).

From the figure, it may be observed that for production ratios below 1 (10^0 in the figure), simulation results suggest that SIT is almost completely ineffective for all release intervals and numbers of release sites. Since a production ratio of 1 indicates that the number of sterile males produced per week per unit area is equal to the equilibrium population of healthy males per unit area, this result tentatively suggests the existence of a threshold time interval (approximately one week in this model) across which the volume of sterile males released must exceed the equilibrium size of the healthy male population in order for an SIT strategy to be effective.

It can also be observed that in all cases, whether the healthy population has been eradicated or not, if all other release options are held constant, above a certain threshold production ratio, even dramatic increases in the volume of sterile male releases have little to no effect on the resulting effectiveness of SIT, as measured by the long-term mean healthy population per hectare. Depending on the release interval and the number of release sites, this threshold value is broadly observed to lie somewhere between 10^1 and 10^2, indicating overall sterile male production per week per unit area of between 10 and 100 times the equilibrium size of the healthy male population per unit area. This effect may be due to density dependent mortality of sterile males, as discussed in Section 6.2.

Whatever the causes, if the observed effects are replicated in real world applications of SIT, identifying these threshold values would be extremely important in avoiding both futile underproduction and costly and ineffective overproduction of sterile insects.

7. Discussion of the model

Since the model presented in this paper was designed to replicate the spatial dynamics of an SIT programme in a simple manner,

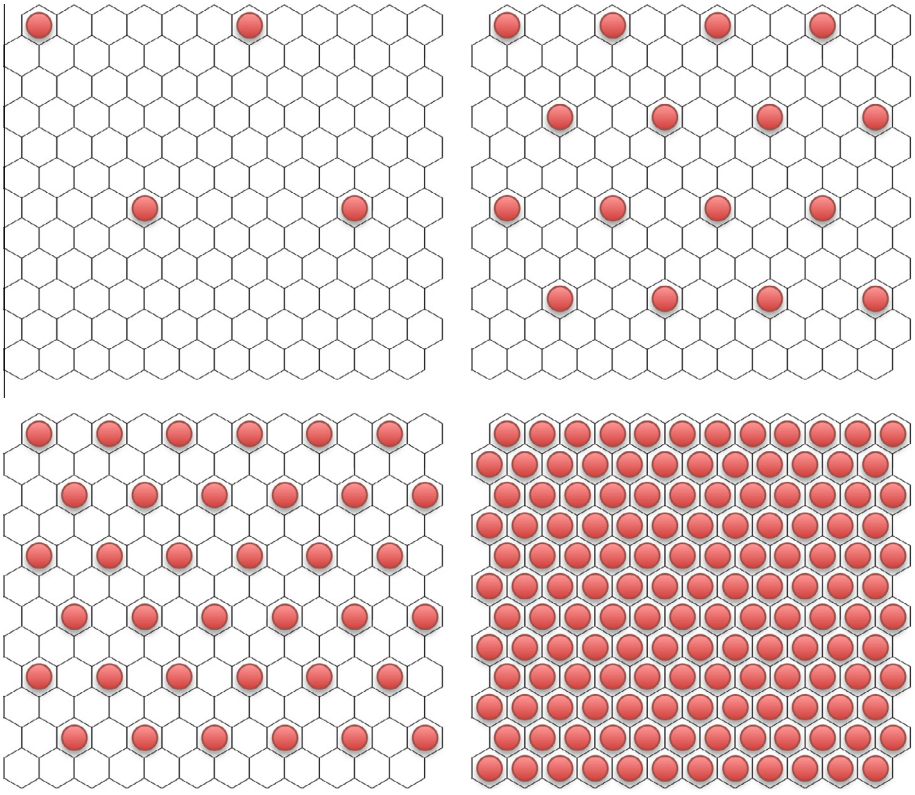

Fig. 12. The four equilateral triangular lattice patterns that can be superimposed on the simulation grid.

there are clearly a number of ways in which it could be adapted, extended and improved.

Regarding the modelling of the dispersal of *Aedes aegypti* as a random walk, some studies have suggested that this may not be justified. From research with honeybees, [54] suggest that flying insects may search for food using a Lévy flight pattern, while dispersal studies of *Aedes aegypti* indicate that females preferentially move towards more highly shaded and vegetated areas with high concentrations of suitable breeding sites and that they avoid crossing busy roads [48]. Also, the model does not explicitly consider the availability of food (human blood in preference [9]), which might be expected to have a significant effect on mosquito movement. It may therefore be beneficial to incorporate a more detailed representation of mosquito dispersal (that proposed by [20], for example) into future versions of the model, in which individuals preferentially move towards more attractive locations (e.g. more highly populated areas or those with higher concentrations of oviposition sites), by adding spatially dependent biases to the random walk process.

The consideration of mosquito densities rather than explicitly counting individuals may also give rise to misleading conclusions. In the model, since mosquito populations are not required to take integer values, the healthy population of a cell may recover from levels close to zero, when in reality a population of less that one should indicate eradication. Therefore, some strategies may be more effective than the model would suggest. This issue could be addressed by rounding all populations to the nearest integer or by considering an equivalent agent-based model.

It is further noted that several of the simplifying assumptions of the model, such as the immediate introduction of sexually mature offspring following fertilisation, may not be reasonable, since the validity of models that do not fully take into account the complex life-cycle of *Aedes aegypti* has been called into question [40]. In particular, it has been observed that density dependent mortality in the species operates particularly strongly at the larval stage of development, and both experimental and theoretical studies have concluded that reducing the number of individuals present at this stage (for example, as the result of an SIT programme) may actually result in an increase in the size of the adult population [55,34], potentially necessitating far more detailed modelling of the processes of hatching and development than is present in the model considered here [18]. Again, this suggests that it may be beneficial to extend the current model, either through the introduction of a time delay between fertilisation and the introduction of mature offspring or through explicit modelling of the immature stages of the insect's life cycle.

It may also be beneficial to re-examine those parameter values used in the model that relate directly to the biology of *Aedes aegypti*. In particular, it would be desirable to determine a reasonable value for the ratio $\hat{m}$ of healthy males to healthy females at which females may reproduce at their maximum biological rate. Evidence suggests that the correct value may be smaller than that used in our simulations, since male mosquitoes of the related species *Aedes albopictus* have been described as "sexually very active" and are capable of mating with 8–9 females per day [43].

However, key features of the dynamics described in this paper do match those reported in other work, such as the observed localised eradication and recolonisation processes, and it is therefore hoped that the model provides a sufficiently faithful representation of SIT such that the broad conclusions drawn regarding release strategies may prove valuable in informing future modelling and field studies.

As noted in Section 5, the parameter values used in the simulations have been drawn from multiple sources and are not intended to be definitive, but are rather considered to be sensible estimates with which to calibrate the model such that general conclusions can be drawn. As discussed, several of the parameters, particularly the birth rate ($\hat{b}$) and the parameter governing the equilibrium

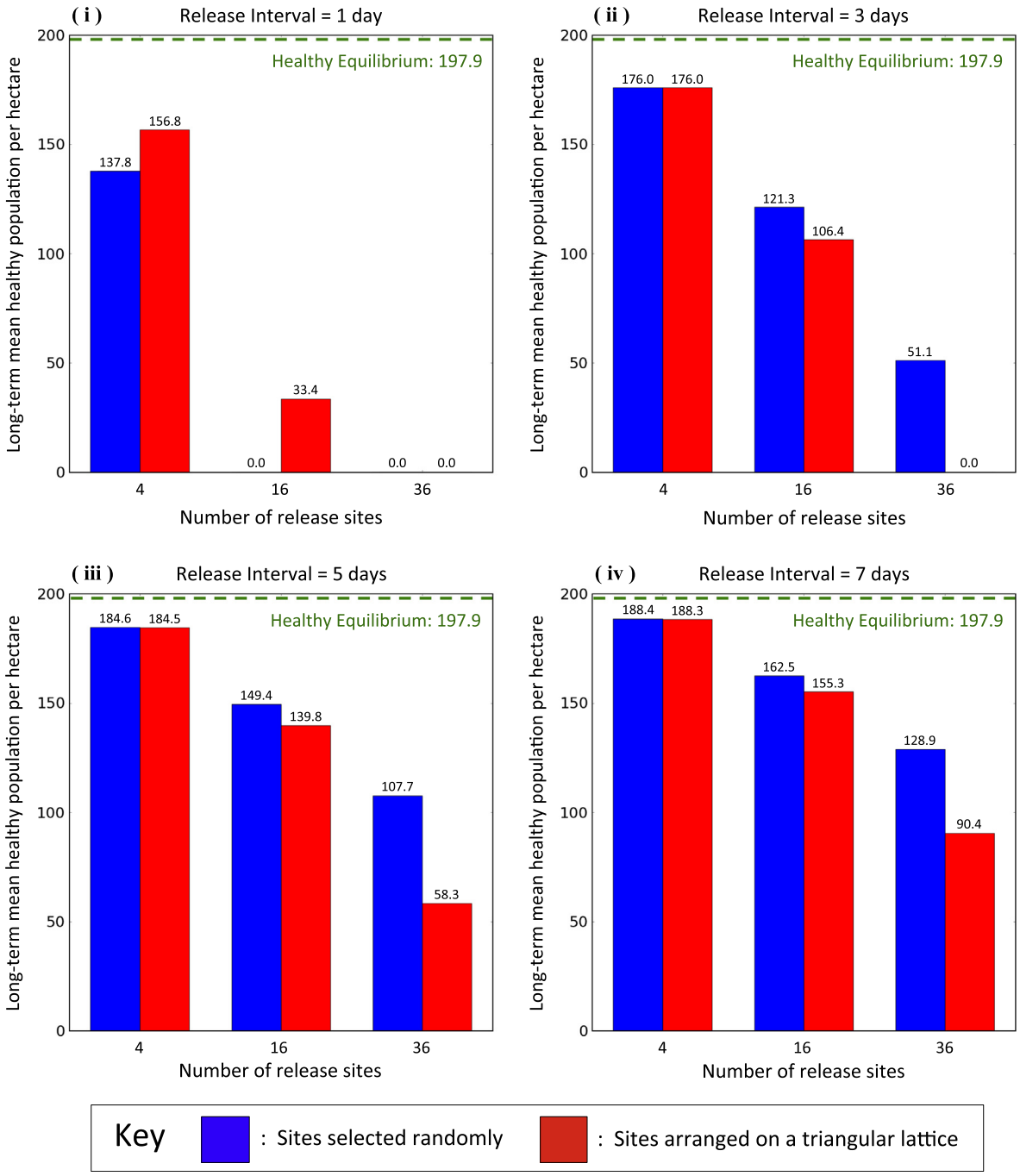

Fig. 13. Comparison of spatially random and fixed lattice sterile insect release patterns on the long-term size of the healthy population. The dotted line indicates the equilibrium healthy population of approximately 197.9 insects per hectare.

density of healthy mosquitoes (C) would be expected to vary depending on terrain, temperature or other factors.

Two further potential technical criticisms of the model dynamics should also be acknowledged. Firstly, the form of the function F was chosen to satisfy particular conditions rather than to reflect the biological properties of *Aedes aegypti*, and the choice may not therefore be justifiable. Secondly, the decision to model dispersal, mortality and reproduction sequentially rather than simultaneously (though also seen in other models) may be a weakness. A careful analysis of the model against data from field studies would be required to determine the validity of these simplifications.

A more subtle potential weakness of this model (and indeed with the modelling of SIT strategies more generally) concerns the extent to which mating preference may be genetically determined in *Aedes aegypti*. Mating preference can be considered to be a "labile trait", whose expression may exhibit considerable phenotypic variation across the species and phenotypic plasticity (environmental dependence) within or between individuals (see, for example, [56–58]). If there is a genetic predisposition of certain females to mate with sterile males, the rate of such matings would be expected to drop over the course of an SIT programme as the relevant genotype becomes more rare, resulting in a corresponding drop in the effectiveness of the control strategy over time.

There is plenty of scope for further mathematical analysis of the model. For example, it may be of interest to investigate the existence of spatially uniform forced equilibria and forced oscillations, in which a fixed number of sterile males are introduced to every cell at regular intervals. It may also be possible to investigate the

continuous limit of the model as the spatial and temporal intervals tend to zero, potentially replacing the discrete model with a set of partial differential equations. The relatively fine spatial scale of the model would also allow for the examination of a wider variety of sterile insect release patterns (see Appendix A).

Of immediate value would be a deeper analysis of the impact of density dependent mortality of sterile males on the effectiveness of SIT programmes, as discussed in Section 6.2. Such analysis would serve both to confirm density dependent mortality as the cause of the observed effects and then to identify the optimal spatial separation of release sites and interval between pulsed releases and the appropriate volume of sterile male production such that this problem is minimised.

It would also be of interest to attempt to apply the model to a specific region where an SIT programme could be undertaken, allowing C to vary spatially to reflect the suitability of the terrain as a habitat for *Aedes aegypti*, tuning the other parameters to fit data collected on mosquito populations in the region and introducing a variable birth rate $\hat{b}$ to correspond to seasonal conditions.

8. Conclusions

Our goal was to create a simple spatially explicit model that would replicate the essential features of SIT in *Aedes aegypti* and to use it to compare different release strategies in terms of the volume of sterile insects released, the number of releases sites and the interval between pulsed releases, factors that had not previously been considered in combination. The model dynamics of a healthy mosquito population were analysed, with the location and stability of equilbria determined and bifurcations identified as the reproductive rate of the species was allowed to vary.

Despite the reservations outlined in Section 7, the following general results from the model can be advanced as indications of which release strategies may be most effective in using SIT to control populations of *Aedes aegypti*, and of the issues that should be considered when planning such control programmes:

1. Given a fixed quantity of sterile males available for release per unit of time for a given area, increasing the frequency of releases and the number of release sites improves the effectiveness of an SIT programme. This was consistently demonstrated by simulations (see Section 6.3). The maximum release interval and minimal number of sites required to eradicate the healthy population should be confirmed by field trials to avoid unnecessary expense.
2. Again, for a fixed quantity of sterile males available for release per unit of time for a given area, there may be a threshold release interval, above which the efficiency per release site of SIT is reduced and eradication of the target species may be unattainable (see Fig. 10). The existence and value of this threshold would also need to be determined by field trials and may be expected to depend on the density of the healthy population.
3. After the cessation of an SIT programme that has not completely eradicated a population of *Aedes aegypti*, or in the periods between insufficiently regular pulsed sterile insect releases, a healthy mosquito population may be expected to rapidly return to its equilibrium value. A key factor behind this effect appears to be the recolonisation of areas of low population density from areas of higher population density that were less affected by SIT, driven by mosquito dispersal (see Section 6.2).
4. Density dependent mortality of sterile males may lead to reduced SIT efficiency if insects are released in large groups (see Section 6.2). Understanding this effect could allow for a reliable cost-benefit analysis of different SIT strategies to be performed in terms of the number and separation of release sites, the interval between pulsed releases and the overall rate of sterile male production.
5. A threshold value may be identified on the overall rate of sterile male release per unit area, in terms of the ratio of sterile males released per unit time to the size of the population of healthy males at equilibrium, above which no further gains in SIT effectiveness can be obtained (see Section 6.4). This highlights the risk of costly and ineffective overproduction of sterile insects. Again, the existence and value of this threshold would need to be determined by field trials and may be expected to depend on the density of the healthy population.

Comparing these conclusions with those drawn from the recent work of Dufourd and Dumont [42,43], one of very few other models to combine pulsed releases with a spatially explicit examination of SIT strategies, we note that, despite the relative simplicity of our modelling approach, our work supports their conclusions on several key points. Firstly, our first conclusion, that increasing the frequency of pulsed releases and the number of release sites leads to improved efficiency of an SIT programme, is in line with their findings and with those drawn from non-spatial models such as those of White et al. [40] and Dumont and Tchuenche [41]. Our third conclusion, that a healthy mosquito population may be expected to rapidly return to its equilibrium value on the cessation of an SIT programme, also echoes the findings of Dufourd and Dumont [43], and is in line with the those of other authors regarding local extinction and recolonisation processes [16,17,29,34].

More broadly, all of the results presented in this article (including the brief comparison of spatially random and spatially uniform release patterns, presented in Appendix A) provide firm support for the principle that "it is necessary to consider a spatio-temporal model to obtain realistic simulations and to simulate several vector control strategies..." Dufourd and Dumont [42] and we hope that this will inform the direction of future research in the field.

Acknowledgements

The authors acknowledge the financial support of the UK Engineering and Physical Sciences Research Council (EPSRC) under the grant ENFOLD-ing - Explaining, Modelling, and Forecasting Global Dynamics, reference EP/H02185X/1.

Thanks are due to the anonymous reviewers for their many constructive comments and to Professor Sir Alan Wilson and Doctor Adam Dennett of the Centre for Advanced Spatial Analysis (CASA) at University College London for the benefit of their observations and suggestions.

T. P. Oléron Evans would also like to thank Elizabeth Swan, Dennis Barnett and Julie Woodhouse for their many years of dedication to developing mathematical understanding, without whom this work would not have been possible.

Appendix A. Alternative release patterns

Using a similar method to that of Section 6.3, further runs were performed to compare the effectiveness of the random spatial release strategy with a strategy of fixed release locations arranged in an equilateral triangular lattice. Given the way in which opposite edges of the simulation zone are connected, 4 such lattice patterns are possible, involving $4, 16, 36$ and 144 release sites, as shown in Fig. 12. Naturally, the lattice of 144 release sites coincides with the random strategy and will therefore be disregarded.

Fig. 13 shows the long-term mean healthy mosquito populations per hectare calculated from simulations of SIT programmes with various release intervals, both for the random spatial release

strategy and the fixed lattice release strategy. As in Section 6.3, each column represents an average over the final 119 or 120 of 300 iterations, across 10 independent runs of the model. Note that those runs conducted with fixed release sites are deterministic and hence the results show no variation. Standard deviation bars have been omitted from the columns representing the random release strategy, since variation was negligible compared to the scale of the graph.

A clear discrepancy can be observed between the results of runs with a release interval of 1 day and those with greater release intervals. In the latter case, the strategy involving a fixed lattice of release sites is consistently more effective at reducing the size of the healthy population. Furthermore, this benefit is observed to increase for higher numbers of release sites. However, in the former case, the reverse seems to be true, with the random strategy outperforming the lattice strategy.

These results suggest that a random release strategy may be more effective for very short pulsed release intervals, while a fixed lattice strategy may be more effective for greater intervals. Unfortunately, geometric limitations of the model preclude a more detailed analysis, since no other equilateral triangular lattices can be described that are consistent with the boundary conditions of the region and the scale is sufficiently coarse that approximations to regular lattices would not be expected to produce reliable results. The observed results may merely be an artefact of the geometry of the simulation region and far more work would be required to draw firm conclusions about the most effective spatial release patterns.

In future work, it may be beneficial to investigate a wider variety of release patterns. In particular, a cycle of fixed offset equilateral lattice patterns of release sites may outperform both of the patterns considered here.

The only previous work known to the authors that has attempted to compare randomly distributed and evenly spread patterns of release sites in a similar way is that of Legros et al. [36], although in their work, randomly chosen sites were picked at the start of a simulation and did not change throughout the duration of a model run. They concluded that strategies involving randomly chosen sites were less effective at reducing the size of the target population than those involving evenly spread sites, broadly agreeing with the results presented here for simulations with release intervals greater than one day. However, since releases in their model occurred at intervals of one week only, it is not known whether the performance of their random strategy would have improved in scenarios with more frequent releases, as observed here.

References

[1] L. Alphey, M. Benedict, R. Bellini, G. Clark, D. Dame, M. Service, S. Dobson, Sterile-insect methods for control of mosquito-borne diseases: an analysis, Vector-Borne Zoonot. Dis. 10 (3) (2010) 295.

[2] T. Shelly, D. McInnis, Road test for genetically modified mosquitoes, Nat. Biotechnol. 29 (11) (2011) 984.

[3] M.Q. Benedict, A.S. Robinson, The first releases of transgenic mosquitoes: an argument for the sterile insect technique, Trends Parasitol. 19 (8) (2003) 349.

[4] C.P. Ferreira, H.M. Yang, L. Esteva, Assessing the suitability of sterile insect technique applied to Aedes aegypti, J. Biol. Syst. 16 (4) (2008) 565.

[5] A.F. Harris, D. Nimmo, A.R. McKemey, N. Kelly, S. Scaife, C.A. Donnelly, C. Beech, W.D. Petrie, L. Alphey, Field performance of engineered male mosquitoes, Nat. Biotechnol. 29 (11) (2011) 1034.

[6] Python Software Foundation, Python Programming Language – Official Website. <www.python.org>, 2012 (accessed 6.6.2012).

[7] NumPy Developers, NumPy. <http://numpy.scipy.org>, 2012 (accessed 6.6.2012).

[8] J.D. Hunter, Matplotlib: a 2D graphics environment, Comput. Sci. Eng. 9 (3) (2007) 90.

[9] M. Otero, H.G. Solari, N. Schweigmann, A stochastic population dynamics model for Aedes aegypti: formulation and application to a city with temperate climate, Bull. Math. Biol. 68 (8) (2006) 1945.

[10] M.H. Birley, Estimation and simulation of variable developmental period, with application to the mosquito Aedes aegypti (L.), Res. Popul. Ecol. 21 (1) (1979) 68.

[11] D.A. Focks, D.G. Haile, E. Daniels, G.A. Mount, Dynamic life table model for Aedes aegypti (Diptera: Culicidae): analysis of the literature and model development, J. Med. Entomol. 30 (6) (1993) 1003.

[12] United Nations Framework Convention on Climate Change (UNFCCC) Secretariat, Stratus Consulting Inc., Compendium on Methods and Tools to Evaluate Impacts of, and Vulnerability to, Climate Change, Final draft report – CIMSiM and DENSiM (Dengue Simulation Model). <http://unfccc.int>, 2005 (accessed 1.3.2014).

[13] M. Maguire, C. Skelly, P. Weinstein, J. Moloney, Simulation modelling of Aedes aegypti prevalence, an environmental hazard surveillance tool for the control of dengue epidemics, Int. J. Environ. Health Res. 9 (4) (1999) 253.

[14] C.R. Williams, P.H. Johnson, S.A. Long, L.P. Rapley, S.A. Ritchie, Rapid estimation of Aedes aegypti population size using simulation modeling, with a novel approach to calibration and field validation, J. Med. Entomol. 45 (6) (2008) 1173.

[15] C.W. Morin, A.C. Comrie, Modeled response of the West Nile virus vector Culex quinquefasciatus to changing climate using the dynamic mosquito simulation model, Int. J. Biometeorol. 54 (5) (2010) 517.

[16] S.A. Ritchie, C.L. Montague, Simulated populations of the black salt marsh mosquito (Aedes taeniorhynchus) in a Florida mangrove forest, Ecol. Modell. 77 (2–3) (1995) 123.

[17] M. Otero, N. Schweigmann, H.G. Solari, A stochastic spatial dynamical model for Aedes aegypti, Bull. Math. Biol. 70 (5) (2008) 1297.

[18] V.R. Aznar, M. Otero, M. Sol De Majo, S. Fischer, H.G. Solari, Modeling the complex hatching and development of Aedes aegypti in temperate climates, Ecol. Modell. 253 (2013) 44.

[19] M. Legros, K. Magori, A.C. Morrison, C. Xu, T.W. Scott, A.L. Lloyd, F. Gould, Evaluation of location-specific predictions by a detailed simulation model of Aedes aegypti populations, Plos One 6 (7) (2011).

[20] A. Mageni Lutambi, M.A. Penny, T. Smith, N. Chitnis, Mathematical modelling of mosquito dispersal in a heterogeneous environment, Math. Biosci. 241 (2) (2013) 198.

[21] S.J. de Almeida, R.P. Martins Ferreira, A.E. Eiras, R.P. Obermayr, M. Geier, Multi-agent modeling and simulation of an *Aedes aegypti* mosquito population, Environ. Modell. Softw. 25 (12) (2010) 1490.

[22] A.M. Ellis, A.J. Garcia, D.A. Focks, A.C. Morrison, T.W. Scott, Parameterization and sensitivity analysis of a complex situation model for mosquito population dynamics, Dengue Transm. Their Control Am. J. Trop. Med. Hyg. 85 (2) (2011) 257.

[23] D.H. Barmak, D.O. Dorso, M. Otero, H.G. Solari, Dengue epidemics and human mobility, Phys. Rev. E 84 (1) (2011).

[24] M. Otero, H.G. Solari, Stochastic eco-epidemiological model of dengue disease transmission by Aedes aegypti mosquito, Math. Biosci. 223 (1) (2010) 32.

[25] C. Favier, D. Schmit, C.D.M. Müller-Graf, B. Cazelles, N. Degallier, B. Mondet, M.A. Dubois, Influence of spatial heterogeneity on an emerging infectious disease: the case of dengue epidemics, Proc. Roy. Soc. B 272 (1568) (2005) 1171.

[26] A. Tran, M. Raffy, On the dynamics of dengue epidemics from large-scale information, Theor. Popul. Biol. 69 (1) (2006) 3.

[27] C.F. Curtis, N. Lorimer, K.S. Rai, S.G. Suguna, D.K. Uppal, S.J. Kazmi, E. Hallinan, K. Dietz, Simulation of alternative genetic control systems for Aedes aegypti in outdoor cages and with a computer, J. Genet. 62 (3) (1976) 101.

[28] Y. Itô, Model of sterile insect release for eradication of melon fly, Dacus cucurbitae COQUILLETT, Appl. Entomol. Zool. 12 (4) (1977) 303.

[29] Y. Itô, H. Kawamoto, Number of generations necessary to attain eradication of an insect pest with sterile insect release method – model study, Res. Popul. Ecol. 20 (2) (1979) 216.

[30] H. Barclay, M. Mackauer, The sterile insect release method for pest-control – a density-dependent model, Environ. Entomol. 9 (6) (1980) 810.

[31] G.W. Harrison, H.J. Barclay, P. van den Driessche, Analysis of a sterile insect release model with predation, J. Math. Biol. 16 (1) (1982) 33.

[32] L. Esteva, H.M. Yang, Mathematical model to assess the control of Aedes aegypti mosquitoes by the sterile insect technique, Math. Biosci. 198 (2) (2005) 132.

[33] N. Alphey, L. Alphey, M.B. Bonsall, A model framework to estimate impact and cost of genetics-based sterile insect methods for dengue vector control, Plos One 6 (10) (2011).

[34] L. Yakob, M.B. Bonsall, Importance of space and competition in optimizing genetic control strategies, J. Econom. Entomol. 102 (1) (2009) 50.

[35] L. Potgieter, J.H. van Vuuren, D.E. Conlong, A reaction–diffusion model for the control of Eldana saccharina Walker in sugarcane using the sterile insect technique, Ecol. Modell. 250 (2013) 319.

[36] M. Legros, C. Xu, K. Okamoto, T.W. Scott, A.C. Morrison, A.L. Lloyd, F. Gould, Assessing the feasibility of controlling aedes aegypti with transgenic methods: a model-based evaluation, Plos One 7 (12) (2012).

[37] V.S. Manoranjan, P. van den Driessche, On a diffusion-model for sterile insect release, Math. Biosci. 79 (2) (1986) 199.

[38] X. Li, X. Zou, On a reaction-diffusion model for sterile insect release method with release on the boundary, Discrete Contin. Dyn. Syst. – Ser. B 17 (7) (2012) 2509.

[39] C. Isidoro, N. Fachada, F. Barata, A. Rosa, Agent-based model of Aedes aegypti population dynamics, in: Lopes, L.S., Lau, N., Mariano, P., Rocha, L.M. (Eds.), 14th Portuguese Conference on Artificial Intelligence Progress in Artificial

Intelligence, Proceedings, vol. 5816 of Lecture Notes in Artificial Intelligence, 2009, pp. 53–64, ISBN:978-3-642-04685-8, ISSN:0302-9743.
[40] S.M. White, P. Rohani, S.M. Sait, Modelling pulsed releases for sterile insect techniques: fitness costs of sterile and transgenic males and the effects on mosquito dynamics, J. Appl. Ecol. 47 (6) (2010) 1329.
[41] Y. Dumont, J.M. Tchuenche, Mathematical studies on the sterile insect technique for Chikungunya disease and Aedes albopictus, J. Math. Biol. 65 (5) (2012) 809.
[42] C. Dufourd, Y. Dumont, Modeling and simulations of mosquito dispersal. The case of Aedes albopictus, Biomath 1 (2) (2012).
[43] C. Dufourd, Y. Dumont, Impact of environmental factors on mosquito dispersal in the prospect of sterile insect technique control, Comput. Math. Appl. 66 (9) (2013) 1695.
[44] P.N. Daykin, F.E. Kellogg, R.H. Wright, Host-finding and repulsion of Aedes aegypti, Canadian Entomol. 97 (3) (1965) 239.
[45] J. Monod, The growth of bacterial cultures, Ann. Rev. Microbiol. 3 (1949) 371.
[46] L.E. Muir, B.H. Kay, Aedes aegypti survival and dispersal estimated by mark–release–recapture in northern Australia, Am. J. Trop. Med. Hyg. 58 (3) (1998) 277.
[47] P.M. Sheppard, W.W. MacDonald, R.J. Tonn, B. Grab, Dynamics of an adult population of Aedes aegypti in relation to dengue haemorrhagic fever in Bangkok, J. Anim. Ecol. 38 (3) (1969) 661.
[48] R. Russell, C. Webb, C. Williams, S. Ritchie, Mark–release–recapture study to measure dispersal of the mosquito Aedes aegypti in Cairns, Queensland, Australia, Med. Veter. Entomol. 19 (4) (2005) 451.
[49] P. McDonald, Population characteristics of domestic Aedes-aegypti (Diptera–Culicidae) in villages on Kenya coast – 1. Adult survivorship and population-size, J. Med. Entomol. 14 (1) (1977) 42.
[50] J. Arrivillaga, R. Barrera, Food as a limiting factor for Aedes aegypti in water-storage containers, J. Vector Ecol. 29 (1) (2004) 11.
[51] H.B. Morlan, E.M. McCray Jr., J.W. Kilpatrick, Field tests with sexually sterile males for control of Aedes aegypti, Mosquito News 22 (1962) 295.
[52] G.R. Conway, M. Trpis, G.A.H. McClelland, Population parameters of the mosquito Aedes aegypti (L.) estimated by mark–release–recapture in a suburban habitat in Tanzania, J. Anim. Ecol. 43 (2) (1974) 289.
[53] K.T.Z. Xiang, S.R. Bishop, Cellular Automata Model for Free Aeolian Sand Dunes, MSc dissertation – University College London, 2010 (unpublished).
[54] A.M. Reynolds, J.L. Swain, A.D. Smith, A.P. Martin, J.L. Osbourne, Honeybees use a Lévy flight search strategy and odour-mediated anemotaxis to relocate food sources, Behav. Ecol. Sociobiol. 64 (1) (2009) 115.
[55] F. Agudelo-Silva, A. Spielman, Paradoxical effects of simulated larviciding on production of adult mosquitoes, Am. J. Trop. Med. Hyg. 33 (6) (1984) 1267.
[56] C.D. Schlichting, M. Pigliucci, Gene regulation, quantitative genetics and the evolution of reaction norms, Evol. Ecol. 9 (2) (1995) 154.
[57] R. Przybylo, B.C. Sheldon, J. Merilä, Climatic effects on breeding and morphology: evidence for phenotypic plasticity, J. Anim. Ecol. 69 (3) (2000) 395.
[58] J.E. Brommer, Phenotypic plasticity of labile traits in the wild, Curr. Zool. 59 (4) (2013) 485.